THERMODYNAMIC PROPERTIES OF DIAMINO-DIAMIDE LIGAND AS POTENTIAL ANTI-INFLAMMATORY AGENT

A Dissertation submitted to the

UNIVERSITY OF CAPE TOWN

In fulfilment of the requirements for the degree of

MASTER OF SCIENCE

by

SEBUSI ODISITSE
B.Sc. (UB)

Department of Chemistry
University of Cape Town
Rondebosch 7700
South Africa

December 2003

To the memory of my Father

ACKNOWLEDGEMENTS

I would like to express my sincere thanks and appreciations to my supervisor, Professor Graham E. Jackson for all the support I received from him during the course of this work.

I would like to also thank the following;

- Professor Gert Kruger and his group at University of Natal for synthesising the ligand
- Members of staff and fellow students in the Chemistry Department (UCT)
- Fellow members of our research group, Edmund, Shane, Nelisa, John, Siyabonga, and Andre for the encouragements
- Noel Hendricks, NMR operator, for assistance
- Fellow 'homeboys and girls' Moricho, Chuchuchu, Pampiri, Ruu, Sadi, Sewa, Mb, and others for the joy we shared in Cape Town
- My wife, Monica for all the support
- Government of Botswana and Ministry of Health for financial assistance
- And above all, glory, honour and power belong to my God.

ABSTRACT

It has been found that low molecular mass copper(II) complexes are effective in the treatment of rheumatoid arthritis (RA). Increasing the amount of copper associated with low molecular mass ligands in plasma helps to alleviate the symptoms of rheumatoid arthritis. Low molecular weight ligand, 3,5-*bis*[(aminoethyl)ethanediamide]-4-oxahexacyclododecane (PCUA) was investigated using glass electrode potentiometry, UV/Visible spectroscopy, nuclear magnetic resonance spectroscopy, speciation modelling as well as blood plasma modelling.

Protonation and stab lity constants were determined at 25 ^{o}C in 0.15 mol dm^{-3} Cl^{-} (Na^{+}) using glass electrode potentiometry and the ESTA (Equilibrium Simulation for Titration Analysis) library of computer speciation modelling programs. The stability constants were determined for complexation of PCUA with divalent copper(II), zinc(II) and calcium(II).

UV/Visible spectroscopy was used to investigate the structures of the different copper(II) solution species. It confirmed the square planar MN_4 type of coordination for MLH_{-1} species. Unfortunately, it was difficult to obtain spectra for MLH_{-2} species due to a lot of noise/interferences.

Nuclear magnetic resonance spectroscopy was used to check both protonation and complexation of the PCUA. The protonation of the ligand was evidenced by a shift in NMR signal arising from protons attached to neighbouring carbons and, also broadening and shifting of the peaks on complexation with copper(II).

The blood plasma si nulation studies using ECCLES (Evaluation of Constituent Concentrations in Large Equilibrium Systems) computer model showed that PCUA had a reasonable potential to mobilize copper *in vivo*. Zinc(II) and calcium(II) were found to be competitors of copper(II) in blood plasma. The plasma mobilizing index obtained for copper-PCUA system was low for an effective mobilization of copper in the presence of other low molecular mass species in blood plasma.

CONTENTS

GLOSSARY

PCUA	3,5-*bis*[(aminoethyl)ethanediamide]-4-oxahexacyclododecane
5UM	N,N'-*bis*[2-(dimethylamino)-ethyl] ethanediamide
6UM	N,N'-*bis*[2-(dimethylamino)-propyl] ethanediamide
5UH	N,N'-*bis*[aminoethyl] ethanediamide
6UH	N,N'-*bis*[aminoethyl] propanediamide
EDA	1,4,7,10,13-pentaaza-5,9-dioxo-7-N-phenethyltridecade
BIDPAP	1,15-bis(N,N-dimethyl)-5-11-dioxo-8-(N-benzyl)-1,4,8,12,15-pentaazapentadecane
Gly	Glycine
BETA	ESTA task for initial estimates of stability constant values
ESTA	Equilibrium simulation for Titration Analysis
DMARD	Disease modifying antirheumatic drugs
NSAID	Non-steroidal Anti-inflammatory Drugs
RA	Rheumatoid Arthritis
SAARD	Slow acting anti-rheumatic drugs
ACTH	Adrenocorticotropic hormone
ECCLES	Equilibrium of Constituent Concentrations in Large Equilibrium Systems
Pmi	plasma mobilizing index
l.m.w	Low molecular weight
R_H	Hamilton an R-factor
R_{lim}	Hamiltonian R-limit
pH	-Log of the activity of the hydrogen ion
$Log\beta_{pqr}$	Logarithm of the overall stability constant
OBJE	Task to minimise the objective function in terms of the emf
OBJT	Task for optimising parameters with respect to reactant concentrations
TOTL	Task to calculate total concentration
VESL	Task to calculate reactant concentration
BURT	Task to calculate the titrant
ZBAR	Task to calculate the complex formation function
Z-bar	Complex formation function
QBAR	Task to calculate the deprotonation function

Q-bar	Deprotonation function
SPEC	Task to calculate the speciation as a function of the pH
U	Objective function
s-dev	Standard deviation in $\log\beta_{pqr}$ for species pqr

FIGURES AND TABLES

Tables

Figure 1: Structural formulae of ligands discussed in this work

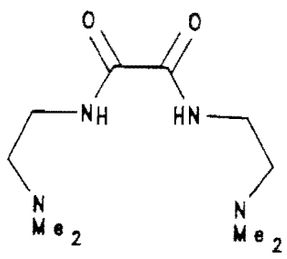

5UM

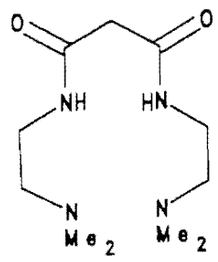

6UM

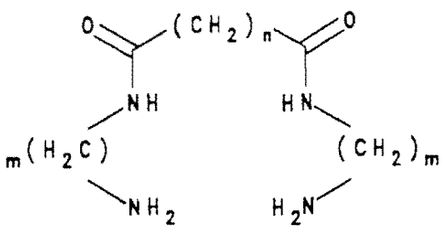

5UH n=0; m=2

6UH n=1; m=2

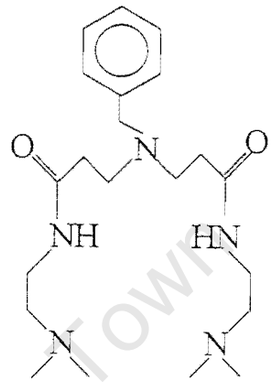

BIDPAP

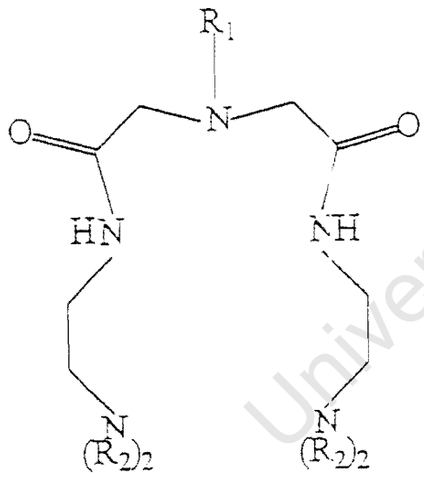

EDA

$R_1 = CH_2CH_2C_6H_5$, $R_2 = H$

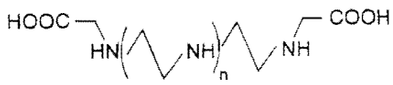

n = 1 DTDA

= 2 TTDA

CHAPTER ONE

INTRODUCTION

1. INTRODUCTION

1.1 RHEUMATOID ARTHRITIS

Rheumatoid Arthritis (RA) is a chronic, inflammatory, systemic disease characterized by joint pain and swelling, joint destruction and pannus formation.[1,2] It is the most common inflammatory arthritis affecting about one percent of the general population worldwide.[3]

RA is one of many chronic diseases that predominate in women. For instance, it has been reported that RA affects 2.1 million Americans and 1.5 million women have RA compared to 600 000 men.[3,4] Onset is usually in the middle age but often in ages of 20's and 30's. The reason for this disease prevalence among women is unknown but presumably it is related to the hormonal milieu.[3-5]

RA remains a major medical challenge because the exact cause of the disease is still not known. However, it is known that RA is an autoimmune disease.[1] The body's natural immune system does not operate as it should resulting in the immune system attacking healthy joint tissue and causing inflammation and subsequent joint damage.

Although RA is properly considered a disease of the joint, it is important to recognize that it can exhibit a variety of extra-articular manifestations.[6] These manifestations clearly show that RA has features of systemic disease capable of involving a variety of major organ systems such as lungs, blood vessels, heart or eyes. Histological studies show that within the rheumatoid synovium, there is hyperplasia of synovial lining cells and development of an intensive network of new blood vessels.[3]

Since the specific pathogenic mechanism of RA is poorly understood, the diagnosis is based upon clinical manifestations or findings. The first indication of this disease is usually polyarthritis affecting the small joints of the hands and feet in a systemic fashion. Large joints and cervical spine may also be involved but the thoracic and lumbar spine are usually spared. The diagnosis may be confirmed by the presence of subcutaneous

rheumatoid nodules, by radiologic demonstration and detection of an antibody in the serum called rheumatoid factor.[6]

1.2 DRUG THERAPY FOR RA

RA is a disease with increased mortality and significant morbidity for which effective therapy interventions are clearly needed.[3] The uses of drug therapy for this disease are the relief of pain, the inhibition of inflammation and the restoration of normal immune mechanisms.[7]

Highly effective drug treatments exist but early treatment is critical for relief of pain, reducing inflammation, stopping or slowing joint damage, and improving patient function and wellbeing. Medications can be divided into two groups: symptomatic and disease modifying drugs.

1.2.1 Symptomatic Drugs

These medications are nonsteroidal anti-inflammatory drugs (NSAIDs), aspirin, analgesics, and glucocorticoids. These drugs help reduce joint pain, stiffness and swelling.

NSAIDs remain an important part of the treatment of RA. They influence pain and inflammation in RA but do not modify the progression of the disease.[8] The traditional example of NSAIDs drugs are Ibuprofen and Diclofenac sodium. The dosage is 1,200 to 3.200 milligrams per day in 3 or 4 doses and 100 to 200 milligrams per day in 2 or 3 doses respectively. Although NSAIDs are effective fighters of both pain and inflammation, gastrointestinal side effects have become the most important complication of chronic therapy with NSAIDs. A number of adverse reactions involving the kidneys has also been associated with the use of NSAIDs.[3]

Because ulcers are potentially dangerous side effect of NSAIDs use, a new option of NSAIDs was recently brought to the market. These are called Cyclooxygenase-2 (COX-2) inhibitors and are safe to the stomach. Although the traditional NSAIDs and COX-2 inhibitors are used, aspirin remains the premier salicylate to be used as an option because of its low cost and potency.

Analgesics play an important role in the treatment of RA. They are mainly for pain relief and are used for patients with mild or intermittent symptoms who do not need regular therapy. One of the most commonly used analgesics is acetaminophen. Unlike NSAIDs, acetaminophen and other pure analgesics do not relieve inflammation. The dosage is 325 to 1000 milligrams every 4 to 6 hours as needed but no more than 4 000 milligrams per day.[9]

Glucocorticoids are also symptomatic medicines. They are sometimes referred to as corticosteroids or simply steroids. Glucocorticoids make up one of the oldest and most commonly used categories of drugs for arthritis. The dramatic effects of cortisone and adrenocorticotropic hormone (ACTH) on the signs and symptoms of active RA were first reported by Dr. Hench and his associates in 1949.[3,10] For many symptomatic rheumatic diseases, these drugs simply work too well yet have too many side effects. The most feared complications in patients with RA have been the effects of steroids on bone and gastrointestinal tract.[3]

1.2.2 Disease Modifying Drugs

The second category of drugs which apparently affect the rheumatoid disease process are disease modifying drugs. These include low doses of methotrexate, leflunomide, D-penicillamine, sulfasalazine, gold therapy, minocycline, azathioprine, hydroxychloroquine (and other antimalarials), cyclosporine and biologic agents. These medications can be further divided into two: disease modifying antirheumatic drugs (DMARDs) and biologic agents.

DMARDs actually stop disease progression before it can cause irreparable joint damage. While DMARDs are powerful arthritis fighters, an instant result should not expected, hence they are also called slow acting antirheumatic drugs (SAARDs).[10]

A widely used and effective DMARDs, which was specifically developed for RA is leflunomide (Arava). Others were approved for RA only after years of use for other purposes. For example, cycloporine was used to prevent organ rejection in people who had undergone transplants. Hydroxychloroquine sulfate was used to treat malaria and methotrexate, one of the most widely used and effective drugs for RA, original used for cancer treatment. People with moderate to severe RA who have not responded well to DMARDs may opt to try protein-A immunoadsorption (*Prosorba*) therapy.

1.3 METAL IONS AND CHELATING AGENTS IN MEDICINE

Metal ions play a vital role in a vast number of widely differing biological processes. These processes are quite specific in their metal ion requirements such that certain metal ions in specific oxidation states fulfill the necessary catalytic or structural requirements. Metal ion dependent processes are found throughout the life sciences and vary tremendously in their function and complexity.[14]

The concentrations of the naturally occurring metal ions in living systems are carefully controlled within fine limits. The interrelationships between metal ions and binding substances in the body are so complex that disorders or disease involving the metal binding substances may result in the presence of high or low concentrations of metal ions compared with that normally present. A number of major diseases are associated with changes in concentration of the trace metal ions in certain tissues and body fluids. It appears that the role of metal ions in medicine can be considered for the following; a). metal poisoning, where excess metal is ingested, b). abnormalities resulting from breakdown of the body's own control system or failure of the metal ion control system and c). the diagnostic analysis of metal ions in the body tissues and fluids.

A trace metal ion that is essential for activity of enzyme systems may be well become toxic if the concentration is raised above certain limits. For example, doubling of the extracellular concentration of potassium ion leads to heart disorders and possibly death. On the other hand accumulation of copper in the tissues, particularly in the liver, brain and kidneys is a result of Wilson's disease. The symptoms may be controlled by penicillamine. Of the metal ions that have been examined, copper appears to be the most valuable pointer to disease conditions. For infectious hepatitis, serum copper levels rise up to three times the normal value due to an accumulation of ceruloplasmin. Other diseases associated with high copper concentrations in the blood are leukaemia, lymphomas, rheumatoid arthritis, psoriasis, cirrhosis, rephritis and Hodgkins's disease.[13-17]

The medicinal aspects of many drugs act via chelation of metal ions. In general drugs act by controlling the action of cells, particularly nerve and muscle cells, by acting on subcellular structures or disturbing enzyme behaviour. The approach in this study is based on the design of copper complexes as anti-inflammatory drug from a bio-inorganic perspective.

References

1. Weyand C.M., *Rheumatology*, 2000, **39**(suppl.1), 3-8.

2. Aeschlinmann A., Simmen B.R., Michel B.A., in: Baumgartner H., Dvorak J., Grob D., Munzinger U., Simmen B.R. (Eds), *Rheumatoid Arthritis*, Thieme Medical Publishers, Inc., New York, 1995.

3. Fischbach M., *Rheumatoid Arthritis*, Churchill Livingstone, New York, 1991

4. Kelly W.N., Harris E.D., Ruddy S., Sledge C.B., *Textbook of Rheumatology*, Vol.1, 5th ed, 1997, W.B Saunders Company, Philadelphia.

5. Maddison P.J., Isenberg D.A., Woo P., Glass D.N., *Oxford Textbook of Rheumatology*, Vol. 2, 1993, Oxford Univ. Press Inc., New York.

6. Melvin J.L., *Rheumatic Disease*, 2nd ed, 1982, F.A. Davis Company, Philadelphia.

7. Wilkens R.F., Dahl S.L., *Therapeutic Controversies in the Rheumatic Diseases*, 1987, Grune and Stratton, Inc. Orlando.

8. Baumgartner H., Dvorak J., Grob D., Munzinger U., Simmen B.R. (Eds), *Rheumatoid Arthritis*, Thieme Medical Publishers, Inc, New York, 1995.

9. Huskisson E.C., *Anti-rheumatic Drugs*, Vol. 3, 1983, Praeger Publishers, East Sussex.

10. Hardin J.G., Longenecker G.L, *Handbook of Drug Therapy in Rheumatic Deseases*, 1st ed, 1992, Little, Brown and Company, London.

11. Schumacher H.R., Gall E.P., *Rheumatoid Arthritis*, J.B.Lippincott Company, Philadelphia, 1988.

12. Utsinger P.D , Zvaifler N.J Ehrlich G.E., *Rheumatoid Arthritis*, J.B.Lippincott Company, Philadelphia, 1995.

13. Ellis G.P., West G.B., *Progress in Med. Chem.* 1980, **17**, 186-260.

14. Hughes M.N., *The Inorganic Chemistry of Biological Processes*, John Wiley and Sons, London, 1974.

15. Williams D.R., *The metals of life*, van Nostrand Reinhold Company, London, 1971.

16. Osterberg R., *Biological role of copper*, Ciba Foundation Symposium 79, 1980.

17. Blumberg W.E., Aisen P., Peisach J., *The Biochemistry of copper*, Academic Press, New York and London, 1966.

CHAPTER TWO

BACKGROUND TO STUDY

2. BACKGROUND TO STUDY

2.1 COPPER AND RHEUMATOID ARTHRITIS

As an essential element, copper plays an important role in all organisms including man. Biologically active oxidation states of copper are (I), (II) and (III). These oxidation states are found in copper complexes that act to transport copper to body sites where it is required. The body gets copper from dietary sources and the richest dietary sources of copper are animal liver, crustacea, shell fish, dried fruits, nuts and chocolate.[1]

Dietary copper is readily absorbed in the stomach and small intestine, from where it is transported to the liver by the blood as a serum albumin complex. In the liver, which is the principal copper processing organ, it is stored as metallothionin complex or converted into ceruloplasmin which is released into the blood to meet normal metabolic needs. Excess copper is excreted via the bile where it is complexed to bilirubin, thereby preventing reabsorption in the gut.[2-4]

Copper is required for haemoglobin synthesis, keratinisation, pigmentation, bone formation, reproduction, fertility, development of central and peripheral nervous systems, cardiac function, cellular respiration, nerve function, extracellular connective tissue formation and regulation of monoamine concentration.[5] Tissue requirements for copper are believed to be met and controlled in a homeostatic fashion based upon availability, absorption, storage, utilization and excretion.[5] All normal tissues contain copper in the form of copper dependent components which include metallo-proteins, metallo-enzymes and lower molecular weight complexes of biological importance.[2-5]

Copper complexes were observed to be effective in the treatment of rheumatoid arthritis and other degenerative connective tissue diseases as early as 1941.[5,21] The elevated serum copper levels during RA, and anti-arthritic properties of copper

compounds led to the hypothesis that endogenous copper might have a protective function in chronic inflammatory conditions. The former copper compounds used in the drugs were cupralene, [Cu(I) (3-allylthiouredobenzoate)] and [Cu(II) 8-hydroxyquinoline (diethylammonium sulphonate$_2$)] also known as dicuprene. Besides these, another treatment of RA was by wearing copper bracelets. It was observed that through sweat, bracelets were solubilised and promoted dermal absorption of copper into the blood stream.[6] The discovery brought about many articles in the literature indicating that copper complexes can be effective in the alleviation of inflammation associated with RA. The search for less expensive, more effective and safer therapies for this disease, and or inflammation associated with it, remains a challenge.

2.2 MECHANISMS OF ANTI-INFLAMMATORY COPPER COMPLEXES [5-7]

Important gains have been made concerning possible biochemical mechanisms of action for copper complexes in relieving inflammation. The possible mechanisms are induction of lysyl oxidase, modulation of prostaglandin synthesis, induction of superoxide dismutase or superoxide dismutase mimic activity, stabilization of lysosomal membranes and modulation of the activity of histamine.

a). Induction of Lysyl Oxidase

Lysyl Oxidase is a copper dependent enzyme responsible for repair of damaged tissues due to inflammation. The process requires cross-linking and extracellular maturation of the connective tissue components, collagen and elastin. It has been observed that lysyl oxidase activity is induced in copper deficient chickens with copper(II) sulphate.

b). Modulation of Prostaglandin Synthesis

Copper complexes have been shown to decrease the synthesis of the pro-inflammatory (vasodilator) prostaglandin, PGE_2 and a concomitant increase in the synthesis of the anti-inflammatory prostaglandin (vasoconstrictor), $PGF_{2\alpha}$.

c). Induction of Superoxide Dismutase and Superoxide Dismutase Mimitic Activity

Rheumatoid Arthritis has been associated with deficiency or lack of superoxide dismutase enzyme activity. The human superoxide dismutase contains copper at the active site and is required for its dismutase activity. The superoxide anion which initiates inflammation, is disproportionated by this enzyme.

d). Stabilization of Lysosomal Membranes

Copper is also found to be important for redox control of human synovial lysosomes. The synovial fluid contains lysosomal enzymes which are destructive towards cartilage. The permeability of lysosomes is found to be decreased by copper and in addition decreased the ratio of free versus bound lysosomal enzymes.

e). Modulation of the Activity of Histamine

Modulation of the physiological effects of histamine may also be an important biochemical role for copper complexes. It is found that copper-histamine complexes are the active form of histamine.

2.3 COMPUTER-BASED APPROACH

The concentration of low molecular weight transition metal complexes is usually very low. These complexes are of immense biological significance because they perform

many roles. They are involved in the transport of metal ions across membrane and between biological binding sites. However, their biological role is not easy to elucidate because they exist well below the limits of analytical means of detection. They are also not amenable to isolation and concentration techniques because these would upset the labile equilibria in which they participate.[8]

A computer simulation of the equilibrium reactions between transition metal ions and low molecular weight ligands was considered to be the only reliable way to determine which of the thousands of possible complexes would be important under biological conditions. Computer simulation in this regard is the calculation of the equilibrium concentrations of the individual species formed in the solutions of metal ions and ligands. It requires the thermodynamic formation constants for all the complexes present in the mixture and the overall concentrations of the components. The computer program called ECCLES, (Evaluation of Constituent Concentrations in Large Equilibrium Systems) was developed to permit the simulation of large and comprehensive systems.[22]

In simulation of data concentration scans are done to ensure that the imposed free concentrations of the metals do not influence their distribution among low molecular weight ligands.[9] In the free metal concentration range that was scanned, the extent of complexation of low molecular weight ligands is far greater than total concentration of metal ligand complexes. This is because of the very low total concentration of the transition metals, the weak bonding abilities of calcium(II) and magnesium(II) and the decrease in metal ion concentration due to protein binding. However, the problem arising from inclusion of protein binding constant in computer simulated blood models are avoided. Computer modeling using ECCLES has provided evidence in support of the hypothesis that the administration of low molecular weight copper complexes would be beneficial in the treatment of RA.[9-11]

The use of chelating drugs to displace the labile copper equilibrium away from plasma albumin in favour of the tissues is the most straight forward way of utilizing

endogenous copper reserves. For this to occur, it requires a drug which is able to compete effectively with the protein for the metal ion and that the predominant metal complex formed in plasma should readily diffuse into the affected synovial tissue. The extent to which administered therapeuticals may be able to fulfil these conditions can be judged by simulating their effects in plasma using ECCLES. In particular a function called Plasma Mobilising Index (P.M.I) is used to ascertain whether the agent is sufficiently powerful and copper specific. Drugs that successfully bind copper *in vivo* in the presence of competing endogenous ligands produce large P.M.I values, which for copper are calculated as follows;[12]

$$(P.M.I)_{Cu} = \frac{\text{Total low molecular weight Cu(II) concentration in plasma in presence of the drug}}{\text{Total low molecular weight Cu(II) concentration in normal plasma}}$$

Based upon the above information, several investigations were carried out by researchers to further the use of copper complexes in alleviation of inflammation and, or RA.

2.4 DESIGNING COPPER(II) COMPLEXES AS ANTI-INFLAMMATORY AGENTS

The *ab initio* design of therapeutic agents usually depends on a knowledge of the difference between health and disease at a molecular level.[8] Although the causes of RA are not yet known, the observed effect of copper on inflammation find the mechanism in which can be utilized in the meantime. Of importance is to find a mechanism in which the supply of copper can be increased at the sites of injury.

The design of RA agents which reduce inflammation is based upon the assumptions that a). the therapeutic effect of copper administration arises from increase in the total

labile copper concentration in the body compartments such as synovial fluid and b). the increase is due to the formation of complexes in plasma that can diffuse into synovial fluid through the separating membrane.

In order to successfully administer and mobilize the metal ion in the body fluids, several general requirements have to be fulfilled. In this case ligands can be used either to mobilize copper from endogenous reserves or exogenous sources, thereby increasing the low molecular mass fraction of copper complexes in the body fluids. The following features would be desirable in a drug design:[13,14]

a). The ligand concerned must be a strong copper complexer in order to form thermodynamically stable species with the metal ion at physiological conditions.

b). The ligand should contain predominantly nitrogen donor groups for high selectivity to copper and that other metal ion equilibria, such as calcium or zinc, are not disturbed in their essential body function.

c). The complex formed must be kinetically labile to be able to liberate and release metal ion at the biologically active site.

d). The complex formed must be formally uncharged and also be lipophilic to enable transport across cell membranes.

e). If the complex is to be administered orally, it ought to have a reasonable low acid dissociation constant so that it can be in an uncharged form at intestinal pH values.

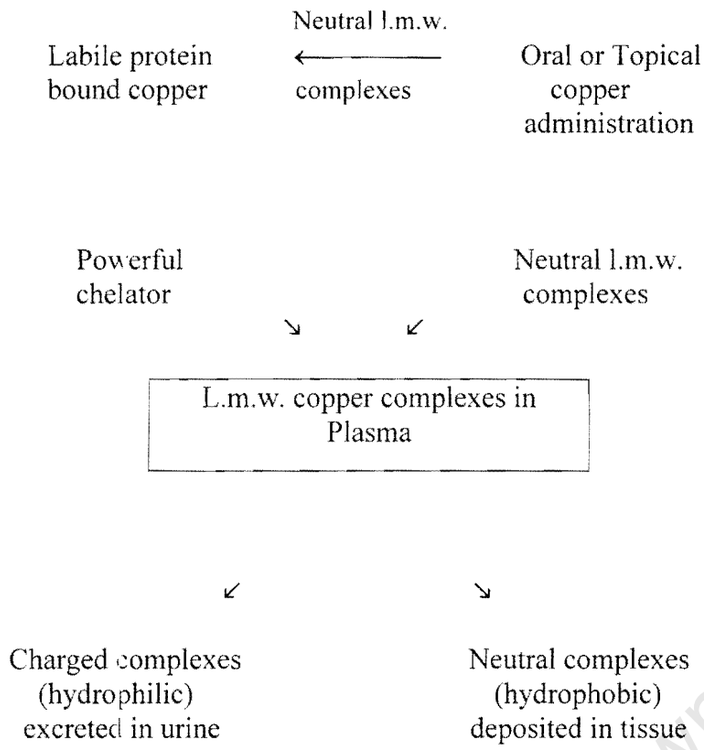

Figure 2.1: Routes for increasing the concentration of l.m.w. copper complexes in blood Plasma.[8]

The increase in the local concentration of copper complexes may be achieved by the two general routes as illustrated in figure 2.1.[8] One is based on the liberation of endogenous reserves while the other on copper supplementation by oral or topical administration. For short term therapy endogenous rather than exogenous sources seem appropriate. This can be achieved by a) equilibrium competition for the labile protein-bound copper, b) decreasing the affinity of serum albumin for copper by allosteric effects and c) extracting copper from inert metalloproteins.

Several ligands have been investigated with copper in trying to fulfill the mentioned requirements. It was found that the copper mobilizing efficiency of a ligand increases as the donor atoms changes from O to S to N.[15] Since the thiol group is toxic, it is not favourable for human therapeutic compounds. Reports show that as the number of

donor atoms in the ligand increases, stability of copper complexes should increase.[18,23] It is also observed that the stability of inorganic chelate complexes is affected by the size of the chelate rings formed upon coordination. For example, 5,6,5 membered chelate system is more stable than 5,5,5 membered chelate system.[16,17,23]

Further investigations were done for 3,6,9,12-tetra-azatetradecanedioic acid (Ttda) and 3,6,9-triazaundecanedioic acid (Dtda). These ligands formed neutral complexes but were found to be highly hydrophilic and easily excreted in urine despite being formally uncharged.[18] The neutrality of the copper complex was achieved by incorporating two acetate groups on the ligand.

In order to increase the lipophilicity of the complex, it was further decided to bury the charge within the ligand. This was achieved by using amides which upon metal coordination lose their protons. The ligands N,N-bis[2-(dimethylamino)ethyl] ethane diamine, (5UM); N.N-bis[2-(dimethylamino)ethyl] propane diamide, (6UM) and N,N-bis [2-(dimethylamino)propyl] ethane diamide were investigated.[14,16] It was found that the copper complexes of these ligands were not neutral at physiological pH. The plasma mobilizing index curves of these ligands showed that these ligands are unable to compete with endogenous ligands hence are poor at mobilizing copper.[19]

The research continued by investigating a series of penta-nitrogen donor ligands. This was done in order to increase both stability and lipophilicity of the complexes. It was found that penta-nitrogen ligands indeed formed more stable complexes than their tetra-nitrogen analoques.[19,20]

The present study is an investigation of a tetra-nitrogen donor ligand system. It has two amino groups and also two amides which upon metal coordination are expected to lose their protons. This system is similar to that studied by Voye.[14,16] The structure of the ligand 3,5-*bis*[(aminoethyl)ethanediamide]-4-oxahexacyclododecane (PCUA) at hand is shown in figure 2.2.

The complex formed is expected to be stable in solution. Of interest in this ligand is the cage moiety attached at the top. This would increase complex lipophilicity and dermal absorption of copper. In addition, the chirality and rigidity of the cage should impose some interesting properties on the ligand.

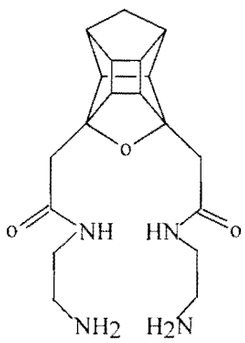

PCUA

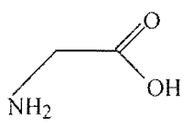

Glycine

Figure 2.2: Structures of PCUA and glycine ligands.

2.5 OBJECTIVES OF THIS STUDY

In order to contribute to the understanding of drug design in the mobilization of copper(II) at the site of inflammation, the thesis had the objectives.

- Determination of the protonation constants of PCUA and the thermodynamic stability constants of this complex with copper(II), zinc(II) and calcium(II) in aqueous solution using glass electrode potentiometry.
- Determination of the structures of the copper complex species using UV/visible spectrophotometry and nuclear magnetic resonance studies.
- Determination of copper plasma mobilizing index for PCUA.

References

1. Delves H.T., in; *Biological role of copper*, Ciba Foundation Symposium 79, Excerpta Medica, Amsterdam, 1980, pp 5-22.

2. Lewis A.J., *Agents Actions*, 1984, **15**, 513.

3. Bremner I., in; *Biological role of copper*, Ciba Foundation Symposium 79, Excerpta Medica, Amsterdam, 1980, pp 23-48.

4. Sorenson J.R.J., *Prog. Med. Chem*, 1989, **26**, 437-547.

5. Sorenson J.R.J., *Prog. Med. Chem*, 1978, **15**, 211-260.

6. Sorenson J.R.J., in; *Metal ions in biological systems, inorganic drugs in deficiency and disease.* (Ed), Sigel H., Mercel Decker, Inc, 1982, **14**, pp 77-113.

7. Hassan M.H., in. *Biological role of copper*, Ciba Foundation Symposium 79, Excerpta Medica, Amsterdam, 1980.

8. May P.M., Williams D.R., in; *Metal ions in biological systems, inorganic drugs in deficiency and disease.* (Ed), Sigel H., Mercel Decker, Inc, 1981, **12.**

9. Jackson G.E., May P.M., Williams D.R., F.E.B.S. Letters, **90**, 1978.

10. Jackson G.E., May P.M., Williams D.R., *J. Inorg. Nucl. Chem.*, 1978, **40**, 1227-1234.

11. Jackson G.E., May P.M., Williams D.R., in; *Metal ions in biological systems, inorganic drugs in deficiency and disease.* (Ed), Sigel H., Mercel Decker, Inc, New York, 1978, **7**, pp 29.
12. May P.M., in; *Handbook of Metal-Ligand Interactions in* Biological *Fliuds, Bioiorganic Chemistry,* (Ed) Berthon G., Mercel Decker, Inc, New York, **2**, pp1184-1201.

13. Jackson G.E., Jarvis N., in; *Handbook of Metal-Ligand Interactions in Biological Fliuds, Bioiorganic Chemistry,* (Ed) Berthon G., Mercel Decker, Inc, New York, **2**, pp 1206-1215.

14. Voye A., *PhD Thesis*, University of Cape Town, 1993.

15. Jackson G.E., Kelly M. J., *J. Inorganica Chimica Acta*, 1988, **152**, 215-217.

16. Jackson G.E., Linder P. Voye A., *J. Chem. Soc. Daltan Trans.*, 1996, 4605-4612.

17. Jackson G.E., Kelly M. J., *Polyhedron,* 1991, **10**, no8, 883-884.

18. Jackson G.E., Kelly M. J., *J. Chem. Soc. Daltan Trans.*, 1989, 2429-2433.

19. Jackson G.E., Gama-M. L., Voye A., Kelly M. J., *J. Inorg. Biochem.*, 2000, **79**, 147-152.

20. Gama-M L., *PhD Thesis*, University of Cape Town, 1999.

21. Sorenson J.R.J, *J. Med. Chem.*, 1976, **19**, 135.

22. May P.M., Linder P.W., Williams D.R., *J. Chem. Soc. Daltan Trans.*, 1977, 588-595.

23. Jackson G.E., in: *Handbook of Metal-Ligand Interactions in* Biological *Fliuds, Bioiorganic Chemistry,* (Ed) Berthon G., Mercel Decker, Inc, New York, **2**, pp 1228-1239.

CHAPTER THREE

GLASS ELECTRODE POTENTIOMETRY

3. GLASS ELECTRODE POTENTIOMETRY

3.1 THEORY

3.1.1 Introduction

Potentiometry is one of the most convenient and successful techniques employed for metal complex equilibrium measurements.[1] Potentiometric methods embrace two major types of analyses. One involves the direct measurement of an electrode potential from which the activity (or concentration) of an active ion may be derived. The other type involves measuring the changes in the electromotive force (emf) brought about by the addition of a titrant to the sample.[2] Analytical chemists design electrodes whose potentials vary in response to changes in the concentration of a specific analyte in solution or in the gas phase.[3]

Glass Electrode Potentiometry (GEP) has found a significant place in the study of many chemical systems in biological, medical and environmental studies.[4] GEP being one of the oldest instrumental methods of analysis, has for the past four decades expanded tremendously.[1] It is preferred because of its high sensitivity, its non-invasiveness and its easy accessibility. However, enhancement in the accuracy and predictability of the values arising from glass electrode potentiometry require a full mastery of the principles behind electrode calibrations.[4]

The easy availability of a glass electrode, its linear Nernstian response, rapid reversibility and high sensitivity to aqueous hydrogen ions over a wide concentration range makes it a suitable technique for the study of equilibria. The classic electrode assembly consists of a pH-indicating electrode and a reference electrode. Typical pH-sensitive glass membranes are either sodium/calcium silicate or lithium silicates with lanthanum and barium ions, which act as lattice tighteners to retard silicate hydrolysis and lessen alkali ion, chiefly sodium ion mobility. The conventional pH electrode has an internal reference electrode (silver/silver chloride or calomel) immersed in a chloride salt buffer (usually a phosphate

at pH 7) solution, with glass membrane separating it from the test solution. The body of the glass electrode is a nonconducting glass tube sealed to a bulb made of special conductive glass which is the pH sensing membrane. The body is filled with a buffered electrolyte of fixed pH value and ionic concentration. This design assures that constant potentials are developed on the inner surface of the glass membrane and on the internal reference element.[2]

In the determination of ligand protonation constants, the ligand solution depending on the initial pH, is titrated with either acid or base in such a way that the pH range of 2 to 11 is scanned. By the inclusion of the metal ion in such a titration, stability constants may upon data analysis, be found.

3.1.2 The Stability Constant

For simplicity, the term "stability constant" or "formation constant" will in this study refer to the values obtained for the overall formation constant of a metal-ligand species. The stability constants provide a quantitative measure of the extent to which a metal will complex with a particular group or ligand. The chemical association of a ligand with protons will then be referred to as the protonation constant.[5]

The position of equilibrium and hence the numerical value of the reported stabibility constant when expressed in concentration units, is normally dependent upon the temperature and the nature of the medium especially the solvent and ionic strength.[6] For any single chemical system studied under a particular set of conditions, different workers may report a range of stability constant values. A set of stability constants may be comparable if they have been measured under similar experimental conditions.

The most accurate and reliable method for the determination of stability constants potentiometrically is to titrate one solution (acid or alkali) with another (of constant total metal and total ligand with alkali or acid), with the potential being determined after each addition of titrant.[7] The study of stability constants essentially involves competition

between two metal ions of which one may be H^+. However, the base titration of aqueous metal-ligand equilibria involves competition between the water molecules, the ligand molecules and hydroxide ions for the metal. The ligand donor sites also attract hydronium ions and metal ions.[1] There may be several pre-complexation processes involved before the final complex species. These would include loss of a coordinated water molecule from the metal, followed by coordination to the ligand molecule accompanied by loss of proton. The overall stability constant is actually the product of stepwise stability constants. However, the constants of the predominant chemical product species are selected to constitute the model that best describes the chemical system.

It is clearly of great importance to be able to assess the factors that influence complex stability.[5] These factors or criteria can be used for the selection of a ligand donor atom for binding of a certain metal ion. Pearson's HSAB (hard and soft acids and bases) principle may be used for the choice of ligand donor atom. According to this theory, a hard donor atom will prefer to bond to a hard accepter atom. If a range of complexes formed by one metal ion is known, Irving-Williams series (Mg<Mn<Fe<Co<Ni<Cu>Zn) may be used to predict the strength of complexes formed by another metal ion in the same series.[8] The known coordination sphere of a metal can also assist in postulating the kind of species that a ligand of a particular denticity will likely form with metal ion, which will also determine the extent to which the complex will be aquated. The concentration ratios of the reactants also influence the species that may predominate at equilibrium.[5,6,8] A high metal to ligand ratio may result in polynuclear species.

The chemical reaction between metal ion M and a ligand L at equilibrium may be represented as;

$$M + L + H \Leftrightarrow MLH \qquad ..3.1$$

Depending on the available parameters pertinent to the system, the stability constant β, may be defined in three ways, thermodynamic, stoichiometric or mixed. It is said to be thermodynamic when expressed with respect to the activity of the reacting species;

$$\beta_{MLH} = a_{MLH} / a_M a_L a_H \quad ..3.2$$

or stoichiometric when expressed with respect to the concentration of the reactants;

$$\beta_{MLH} = [MLH] / [M][L][H] \quad ..3.3$$

It is can also be described as mixed if it is expressed with respect to both the concentration and the activity coefficients interchangeably;

$$\beta_{MLH} = [MLH] / [M][L]a_H \quad ..3.4$$

The ideal thermodynamic stability constant is determined only at an ionic strength equal to zero (I = 0), but this is practically impossible because the reactants species themselves make ionic contribution to the reactant solution.[1,4] It is therefore necessary to measure stability constants at specified constant ionic strength so that comparison can be made when working under similar experimental conditions. It is from this specified constant ionic strength that extrapolation is made to zero ionic strength to obtain thermodynamic stability constants. In this study experimental conditions refer to the ionic strength (I), the temperature (T) and the nature of the background electrolyte.

3.1.3 The Background Medium and Temperature

Whole body investigations must, of necessity be performed in a nutrient medium that supports the life of the organism.[6] However, it is also necessary for a solution chemist to choose working medium conditions for the chemical model. In order to determine stability constants at constant ionic strength, several salts are used for the test solution. These include potassium nitrate (KNO_3), sodium perchlorate ($NaClO_4$), sodium chloride (NaCl), and potassium chloride (KCl). The concept of ionic strength was introduced in 1921 by Lewis and Randall who stated that, 'in dilute solutions, the activity coefficient of a given strong electrolyte is the same in all solutions of the same ionic strength'.[9] It was

since then that many workers attempted to keep activity coefficient constant by using solution of constant ionic strength. For a given chemical system, the background electrolyte is selected such that it a) contributes little to the measured physical property, b) forms very weak complexes with the species under investigation and c) is sufficiently soluble in the solvent used to give ionic medium of the required concentration.

It is desirable to select the electrolyte that yields ions that are common to the reacting acid and base. Basically the anions of the electrolytes are the ones employed to maintain the ionic strength at a constant value. Among the anions of interest, chloride ion has a tendency to form ion pairs. The trend in the tendency to form ion pairs is as follows;[8]

$SO_4^{2-} > Cl^- > Br^- > I^- > NO_3^- > ClO_4^-$

However, it was found that a trend in series of stability constants measured in 3.00 M $NaClO_4$ had values similar to the trend in stability constants measured in 0.15 M NaCl. Therefore, sodium perchlorate is used as a background electrolyte in studying biological systems. In this study sodium chloride would be preferred because human blood is isotonic with 0.15 M NaCl. The other reason is that ClO_4^- has been found to induce problems to the electrode thus resulting in consequential serious impairment in its performance and increasing drift.[1]

The activity **a** of the ion **i** s defined with respect to its activity coefficient **γ** and concentration **c** as follows;

$$a_i = c_i \gamma_i \qquad ..3.5$$

The ionic strength **I** of a solution is defined by the expression;

$$I = 0.5\Sigma c_i z_i^2 \qquad ..3.6$$

where c and z are the concentration and the charge of the ion **i** respectively.

The stability constants are also affected by temperature as represented by the Van't Hoff equation;

$$dlnK/dT = \Delta H^{o}/RT^{2} \quad ..3.7$$

where ΔH^{o} is the standard enthalpy change of reaction and is related to Gibbs free energy ΔG^{o} and entropy ΔS^{o} changes of reaction, T is the absolute temperature in Kelvin and R is the natural gas constant in $JK^{-1}mol^{-1}$.

3.1.4 The Electrode Cell and Glass pH Electrode

In a potentiometric type of sensor, a membrane or sensing surface acts as a half cell, generating a potential proportional to the logarithm of the analyte activity (concentration). This potential is measured relative to an inert reference electrode that is also in contact with the sample or test solution.[2] From the reaction cell, the observed potential is due to the potential difference between the glass electrode and the reference electrode E_{ref}, the potential of the liquid junction of the reference electrode E_{lj} and the potential at the membrane of the glass electrode E_{g}. The reaction cell potential may be represented by the following equation;

$$E_{cell} = E_{g} - E_{ref} + E_{lj} \quad ..3.8$$

The potential of the glass electrode may be written in terms of the activity of hydrogen ion to which it is responding by means of the Nernst equation;

$$E_{g} = E_{g}^{o} + (RT/F)\ln\{H^{+}\} \quad ..3.9$$

where F is Faraday constant, T is the temperature of the system, R is the gas constant, E_{g}^{o} is the standard electrode potential and $\{H^{+}\}$ is the activity of hydrogen ion.

The cell potential may be rewritten as follows;

$$E_{cell} = [E_g^{\circ} + (RT/F)\ln\{H^+\}] - E_{ref} + E_{lj} \quad ..3.10$$

The glass electrode potentiometry employs glass pH electrode which measures the concentration of the hydrogen ions at constant ionic strength. The activity of hydrogen ions becomes a constant at constant ionic strength. Since the concentration of the hydrogen ions is a measurable quantity, the cell potential can be defined by the relationship;

$$E_{cell} = E_{const} + (RT/F)\ln[H^+] \quad ..3.11$$

where RT/F is the Nernstian electrode response slope and E_{const} is a potential dependent on the electrode system used.[4,10]

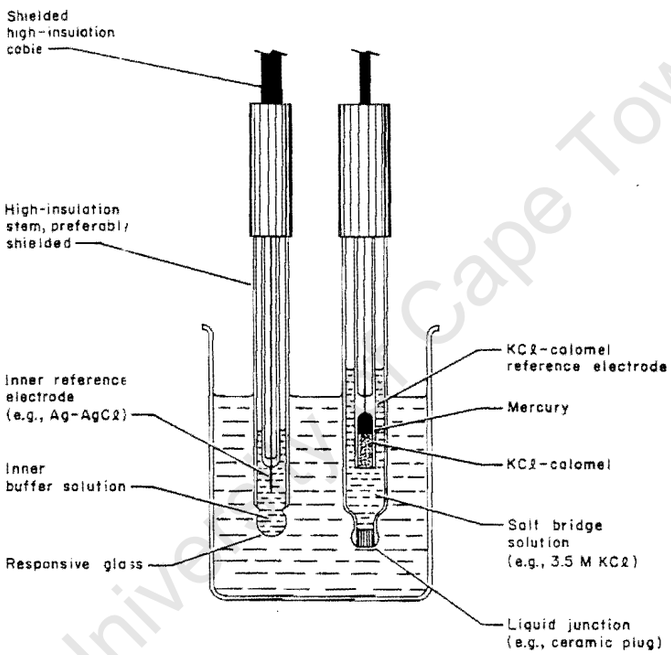

Figure 3.1: Glass indicator – calomel reference electrode cell with liquid junction.[10]

The glass electrode system for potentiometric determination of stability constants is shown in figure 3.1.[10] The glass pH electrode has several constructional components

which are contributors to the overall glass electrode potential. Such components include the inner reference electrode, the inner glass surface, the outer glass surface and asymmetric characteristic of the glass such that a potential may exist across it even when identical solutions are in contact with the inner and outer surfaces. The inner solution which forms part of the inner reference electrode system, is used to provide a stable pH to ensure a constant potential on the inside of the glass. The temperature dependence of the potential response for hydrogen ion activity (concentration) is demonstrated by the slope factor, s, in the Nernst equation;

$$E = E_{const} + s \log[H^+] \qquad .. 3.12$$

The reference electrode is an oxidation/reduction half cell of known and constant potential at a particular temperature.[2] It consists of three principal parts which are an internal element, some filling solution which constitutes the salt-bridge electrolyte and an area in the tip of the electrode that permits a slow, controlled flow of filling solution to escape the electrode called the fluid or liquid junction into the sample. The liquid junction potential at this boundary is considered to arise because of differences in the mobilities of ions carrying opposite charges. It is said to constitute one of the most important and difficult parts of electrochemical measurements with the glass electrode at both theoretical and practical standpoints. The liquid junction potential may be affected by;

- pH and ionic mobility
- ionic strength
- colloids and suspensions
- non aqueous – aqueous boundaries
- the salt bridge solution
- temperature and pressure.

3.1.5 The Basic Equilibrium Systems Equations

The reaction between metal ion, M, and n ligands, L, may be represented with their stepwise equilibrium stability constants as follows;

$$M + L \Leftrightarrow ML \qquad \beta_1 = [ML] / [M][L] = K_1 \qquad .. 3.13$$

.....

$$M + nL \Leftrightarrow ML_n \qquad \beta_n = [ML_n] / [M][L]^n = K_1K_2K_3..K_n \qquad ..3.14$$

where K's are called the stepwise stability constants and β's are called the overall constants.[6]

For a equilibrium system which involves protons, H^+, equation 3.13 becomes:

$$M + L + H \Leftrightarrow MLH \qquad \beta_{MLH} = [MLH] / [M][L][H] \qquad ..3.15$$

However, if the hydroxide ion OH^- emerges in the system then the above equation becomes;

$$M + L + OH \Leftrightarrow ML(OH) \qquad \beta_{ML(OH)} = [ML(OH)] / [M][L][OH] \qquad ..3.16$$

In data analysis, the loss of proton from a metal complex is viewed as similar to the gain of hydroxide ion;

$$M + L \Leftrightarrow MLH_{-1} + H \qquad \beta_{MLH-1} = [MLH_{-1}][H] / [M][L] \qquad ..3.17$$

A comparison of equations 3.16 and 3.17 reveals that the equilibrium constants defined by these two equations may be related to the ionic product of water;[11]

$$\beta_{MLH-1} = \beta_{ML(OH)}[H][OH] = \beta_{ML(OH)} K_W \qquad ..3.18$$

therefore; $\log\beta_{MLH-1} = \log\beta_{ML(OH)} - pK_w$ ..3.19

3.1.6 Computational Data Analysis Theory

The employment of computational analysis comes after the data have been carefully collected in the laboratory. It is then that the unknown parameters are calculated from the accurately measured and known parameters. In this case the unknown parameter of interest is the stability constant. The known parameters may include volumes of reaction solutions, temperature, potential existing in the solution and other parameters.

In a solution of constant ionic strength containing metal ions, M, ligands, L, and protons, H^+, a general equilibrium reaction can take place as described by mass balance equation;[11,12]

$$pM + qL + rH \Leftrightarrow M_pL_qH_r \quad ..3.20$$

where p, q and r are the stoichiometries of the components in the complex.

The equilibrium constant, β_{pqr}, for this reaction is designated as;

$$\beta_{pqr} = [M_pL_qH_r] / [M]^p [L]^q [L]^r \quad ..3.21$$

where [] denotes concentration of species.

The total concentration of the metal, T_M, and of ligand, T_L will be;

$$T_M = [M] + \sum p [M_pL_qH_r] \quad ..3.22$$

$$T_L = [L] + \sum q [M_pL_qH_r] \quad ..3.23$$

where [M] is the concentration of the free aquated metal ions and the summation is over the concentration of all the metal containing species which may be protonated ($r > 0$) or may not ($r = 0$), and [L] is the concentration of the uncomplexed ligand and the summation is over the concentration of all the protonated and unprotonated ligand containing species. It is possible that r may be less than zero ($r<0$) in which case either a proton has been lost from the complex or an hydroxide ion has been added.

In this study the species $M_pL_qH_r$ is denoted by the stoichiometric coefficients p,q,r i.e. 11-1 denotes the complex species MLH_{-1} with r =-1 referring to the removal of a proton from either a coordinated ligand or a bound water molecule or hydroxide ion addition to the complex.[13,14] The $M_pL_qH_r$ can be regarded as protonated complex if $r \geq 1$.

The establishment and the use of mass balance equations ensures that all possible complex species of a system under study are detected and hence their formation constants can be determined..

3.1.7 The ESTA (Equilibrium Simulation of Titration Analysis) Program Library[15]

The program ESTA is a flexible, important computational tool for the determination of protonation and formation constants in aqueous chemical equilibria. The program library is used to calculate equilibrium distributions of chemical species, to analyse potentiometric titration data and to manipulate titration data for a variety of other purposes. The calculations are performed using a Gauss-Newton method to solve the mass balance equations (m.b.e).

The Gauss-Newton method is used to minimize the objective function, **U**, in the ESTA program. The objective function is optimized by the task OBJE within the ESTA2 module. The optimization is done with respect to the observed emf (electromotive force). In contrast, with the OBJT task, optimization is based on total concentrations. Since the variation in total concentrations are smaller than the variation in emf, OBJT is more robust and faster than OBJE but is less sensitive. Thus in practice OBJT would often be

used for initial optimization followed by OBJE for the final optimization. The ESTA program also calculates two important functions which are the formation function, Z-bar, and the deprotonation function, Q-bar. These functions are calculated by the tasks ZBAR and QBAR within ESTA1 module. They are defined differently for the ligand, the binary and the ternary systems. This is because the kinds of equilibria taking place in the different systems may vary depending on the number of the components that constitute each system.

The program ESTA also incorporates the task SPEC in ESTA1 module and this calculates the distribution of species taking part in an equilibrium system as a function of the pH of the solution.

3.1.8 The Objective Function (U)[16]

The objective function, U, may be described as the summation of all the squared residuals of the real parameter values from the calculated values. This function may represented as:

$$U = (N - n_p)^{-1} \sum n_e^{-1} \sum w_{nq} (y_{nq}^{obs} - y_{nq}^{calc})^2 \qquad ..3.24$$

where N is the total number of experimental points,

n_p is the number of parameters being optimized,

n_e is the total number of electrodes,

w_{nq} is the weight of the q^{th} residual at the n^{th} point and

y_{nq} is the electrode emf of the electrode q at the n^{th} point.

The optimization of the resulting data can be achieved by minimization of the objective function. In order to minimize U, a Gauss-Newton approach is employed and this assumes that the function is quadratic with respect to all the parameters. Therefore U can be expressed as;

$$U = \mathbf{a} + \mathbf{p}^t\mathbf{b} + (\mathbf{p}^t\mathbf{H}\mathbf{p})/2 \qquad ..3.25$$

Where **a** and **b** are Gauss-Newton quadratic parameter vectors, **p** is optimization parameter vector, $\mathbf{p}^t$ transpose of **p** and H, the Hessian, is given by:

$$H_{sr} = d^2U / dp_s dp_r \quad ..3.26$$

A well defined system with good initial estimates often converges. The calculations are terminated if the resultant shift vectors are large or if the shift vector has an upward gradient. Once the U is minimized, the standard deviation, the Hamilton R-factor and its limit and the correlation coefficients are then calculated and reported with the optimized values of the stability constants.

3.1.9 The Formation Function (Z-bar) and Deprotonation Function (Q-bar)

The ESTA programs also calculate two important functions from the titration data. These functions are the formation function, Z-bar, and the deprotonation function, Q-bar. These functions are defined differently depending on the presence or absence of a metal ion.

In the absence of a metal ion the protonation function is expressed as;

$$Z_H = (T_H^* - H + OH) / T_L \quad ..3.27$$

where T_H^* is the total hydrogen ion concentration, T_L is the total ligand concentration and $OH = K_W / [H]$. The Z_H function is plotted against pH. The Z_H may be described as the average number of hydrogen ions bound to the ligand at each pH.

The complex formation function, Z_M, measures the average number of ligands bound per metal ion at each concentration of the ligand. This function, Z_M, may be represented as;

$$Z_M = (T_L - [L]) / T_M \quad ..3.28$$

where T_L and T_M are total ligand and metal concentrations respectively, and [L] is the free-ligand concentration. T_L is given by the equation below;

$$T_L = [L] + \Sigma\, q\beta_{pqr}\, [L]^q\, |H]^r \qquad ..3.29$$

The function, Z_M, is pltted against pL, i.e. –log[L].

On the other hand, the deprotonation function, Q_M, is the average number of protons released from the ligand per metal ion as a result of complexation.

$$Q_M = (T_H^* - T_H) / T_M \qquad ..3.30$$

where T_H and T_M are the total proton and metal concentrations respectively, and T_H^* is the calculated total concentration of protons that would be necessary to give rise to the observed pH in the absence of the metal ions or rather if no complexation took place.

$$T_H^* = [H] - [OH] + \Sigma\, r\beta_{pqr}\, [L]^q[H]^r \qquad ..3.31$$

where $[OH] = K_w / [H]$ and the summation is the over all protonated ligand species.

In binary systems, a formation function representing the number of protons that would be on the ligand in the absence of the metal ion, is simultaneously defined as;

$$n_H = (T_H^* - [H] + [OH]) / T_L \qquad ..3.32$$

The difference between n_H and Q_M gives the number of protons on the complex. This can be represented as;

$$r = (q \times n_H) - (Q_M \times p) \qquad .. 3.33$$

where p and q are the stoichiometric coefficients of the metal and the ligand respectively. If p = q = 1, and $n_H = Q_M$, then r = 0 and hence ML species stability constant is given by β_{110}. For r < 0, it is either the deprotonation of the complex formed or the formation of the hydroxo species.

Polynuclear complexes arise whenever there is a ligand capable of bonding to more than one metal ion. Such ligands include hydroxide, carboxylate etc., as well as multidentate ligands that may act in a bridging fashion.

3.1.10 Data Error Analysis

The determination of the protonation and stability constants requires minimal experimental errors. The optimization of stability constants may be affected by the magnitude of random and systematic errors inherent in the system. Therefore a thorough examination of these errors has to be made. This may be done by studying a well known system for experimentally generated error, or by varying the reaction conditions for a particular system and observing its reproducibility.

Random errors usually cancel each other out as the number of titration points increases as opposed to the systematic errors.

3.1.10.1 Weighting[17]

The neglect of weighting can undoubtedly have very detrimental consequences. The purpose of weighting is to reduce as much as possible the adverse influences of optimized parameters that arise because errors in the values held constant during the calculation tend to propagate differently at different points. To obtain unbiased results, the data ought to be weighted so that those points likely to be distorted most by the experimental error are correspondingly reduced in their effects on the optimized values of parameters. The weight may be described as the reciprocal of the variance of the residual between the

observed and the calculated data. The weight of the q^{th} residual at the n^{th} titration point may be expressed as;

$$w_{nq} = [\Sigma \{\delta(y_{nq}^{obs} - y_{nq}^{calc}) / \delta p\}^2 \sigma p^2]^{-1} \quad ..3.34$$

where y_{nq}^{obs} and y_{nq}^{calc} are observed and calculated variables of *q*th residual at *n*th point respectively. σ_p is the standard deviation in the parameter p to be optimized.

If the initial estimates of the optimized parameters are good, an excellent set of weights based on the particular model chosen can be calculated. These weights may be then applied as constants in the subsequent optimization.

After an optimization of the weighted data, the experimental and calculated values of the refined parameter are indicated by the Hamiltonian R-factor. It is represented as;

$$R_f^H = [U / \Sigma n_e^{-1} \Sigma w_{ni} (y_{ni}^{obs})^2]^{0.5} \quad ..3.35$$

The R-factor is compared with the R-limit calculated from;

$$R_{lim}^H = [N / \Sigma n_e^{-1} \Sigma w_{t\,q} (y_{nq}^{obs})^2]^{0.5} \quad ..3.36$$

The R_{lim}^H is the best possible R value based on the random error in the analytical data and the number of variables. Thus the closer R_f^H gets to R_{lim}^H the better the agreement between the theoretical model and the experimental data. However, if $R_f^H < R_{lim}^H$ the model is within the maximum allowed experimental error.[36]

Figure 3.2 on the next page shows a flow diagram for computational procedure employed for the determination of protonation and stability constants by using ESTA library programs.

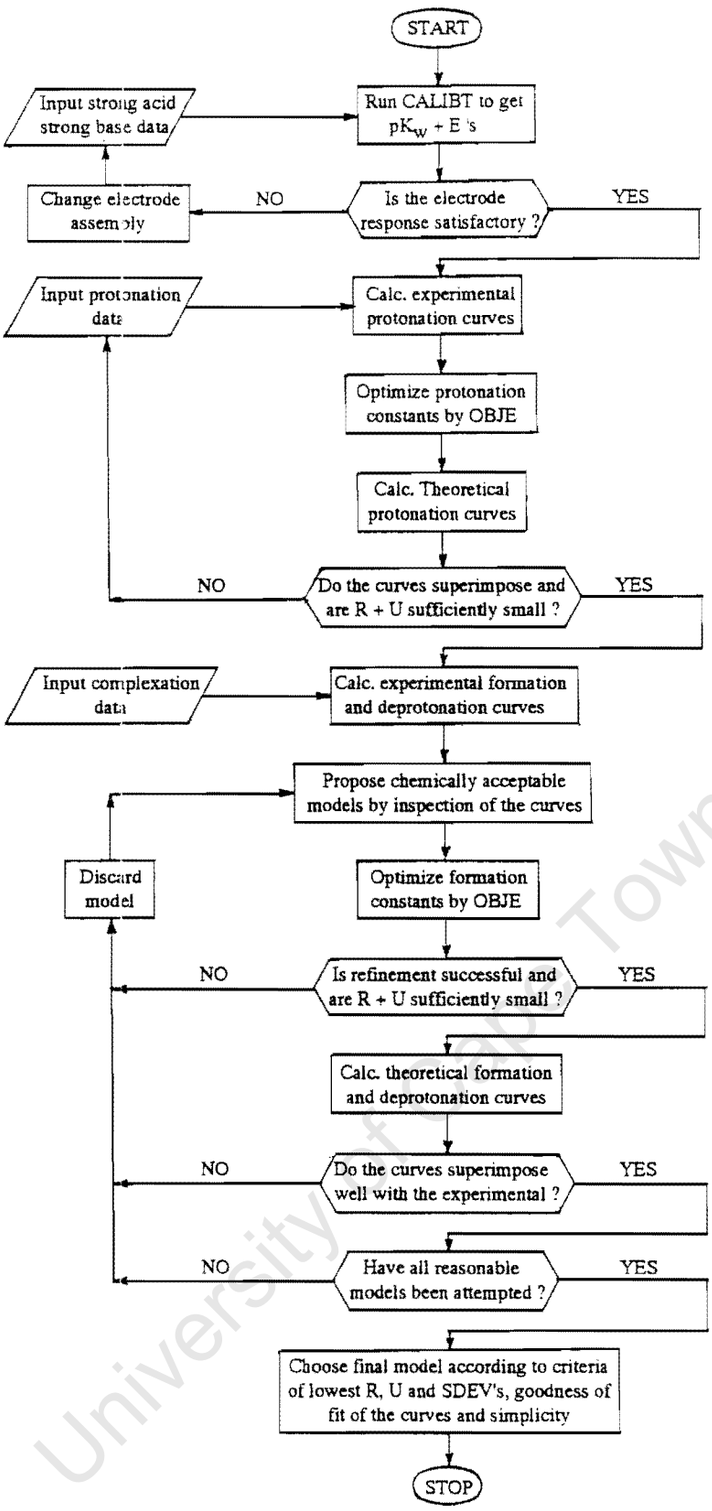

Figure 3.2: Flow chart describing the procedure for the determination of the protonation and complexation constants.[26]

3.2 EXPERIMENTAL

Titrations were performed using a Metrohm 6.0222.100 Combined LL pH glass electrode. The slope of the electrode was calibrated in terms of hydrogen ion activity using buffer solutions of known pH and finally E^0 determined by strong acid - strong base titration at 25 °C. The emf was monitored using a Radiometer PHM 84 Research pH meter. The reaction vessel was kept at a constant temperature of 25 °C by circulating water from a thermostated water bath. Titrant, for example sodium hydroxide solution, was dispensed by the use of Metrohm 665 Dosimat piston burette.

All titrations were performed under an inert condition of nitrogen. The nitrogen was purified by passing it through a series of gas bottles containing, 50% potassium hydroxide to remove carbon dioxide, Fieser's solution to remove oxygen, glass wool, distilled water and background electrolyte solution of ionic strength 0.15 mol/dm^3 (Cl^{-1}) to humidify the gas.[18] The potentiometric titration system was controlled and monitored through a computer.

3.2.1 Preparation of Solutions

All titration solutions were prepared from recrystallized NaCl as background electrolyte, at ionic strength of 0.15 mol/dm^3 (Cl^{-1}). The choice for this ionic strength was based on the fact that human blood is isotonic with 0.15 M NaCl. Prior to preparation of these solutions, the NaCl was dried in a dessicator for at least 24 hours. The solutions were prepared using glass distilled deionised water which has been boiled to remove dissolved carbon dioxide and kept in a container protected by a carbon dioxide trap.

3.2.2 Preparation of Ligand Solution

Solutions of ligand under study were prepared by dissolving accurately weighed samples of glycine and PCUA in the background electrolyte. The estimated concentrations of these solutions were calculated based on the mass of each of the two ligands. The

concentration of glycine solution was approximately 0.01 M and that of PCUA solution was approximately 0.02 M.

3.2.3 Stock Acid Solution (HCl)

Acid solutions of HCl were prepared to a concentration of 0.01 M from Merck ampoules (1.09973 – Titrisol) in background electrolyte. The solutions were standardized against recrystallized sodium tetraborate decahydrate (borax), $Na_2B_4O_7 \cdot 10H_2O$.[18]

3.2.4 Stock Base Solution (NaOH)

The solutions of 0.1 M NaOH were prepared from Merck ampoules (1.09959 – Titrisol) in background electrolyte and also CO_2 free environment to avoid CO_2 contamination. These solutions were stored in bottles fitted with CO_2 traps. Standardisation of these solutions was done against recrystallized potassium hydrogen phthalate.[18] The 0.1 M NaOH solutions prepared were further standardized against 0.01M HCl solutions. This acid – base titrations were also used to check the carbonate content of the sodium hydroxide solution by the use of Gran method.[19]

3.2.5 Metal Ion Solutions

It is very important that the concentrations of standard metal ion solution be as accurate as possible to ensure good data analysis. 0.02 mol/dm^3 solutions of the divalent cations were prepared from $CuCl_2 \cdot 2H_2O$, $ZnCl_2$ and $CaCl_2 \cdot 2H_2O$ in the background electrolyte. These solutions were titrated against 0.01 M standard solution of disodium salt of ethylenediamine tetraacetic acid using the standard methods.[18] Fast sulphon black F (FSB), solochrome black (SB) and methylthymol blue (MTB) indicators were used for the determination of Cu^{2+}, Zn^{2+} and Ca^{2+} ions respectively.

A small amount of HCl was added to the metal ion solutions to prevent the hydrolysis of the metal ions. The acid concentration in the metal solution was determined by

potentiometric titration of 15 ml volume of the metal solution with 0.01 M HCl solution. The Gran method was used to analyze the data obtained.[19,20,21] The acid titration of the metal solution was preferred over the base titration to avoid possible metal hydroxide formation. The formation of the metal hydroxide would give inaccurate concentration of hydrogen ions present in the metal ion solution.

3.2.6 Calibration of Glass Electrode System

Prior to calibration, the electrode was stored in 3 M potassium chloride (KCl) solution at 25 °C. In order to ensure good performance by the electrode, it was placed in acid solution and then base solution for approximately 20 minutes per solution. That was done to ensure sensitivity of the electrode at a wider range of pH from acid to alkaline regions.

The slope of the combined pH glass electrode was determined using commercially available buffer solutions of known pH. These buffer solutions were of pH 4.01, 7.01 and 9.18 and the buffer line was obtained by plotting emf of each pH solution against the pH. The Nernstian slope of the buffer line gave the value of s = 59.15 which was within the acceptable working range of 58.60 to 59.16 at 25°C.

Final calibration of the electrode E_{const} was made from strong acid – strong base titrations at constant ionic strength (I = 0.15 mol/dm^3) and temperature (25 °C). That was done in order to obtain more precise values of s and E_{const} by the introducing the titration data into ESTA library programs.

The calibration of the glass electrode was performed to suit the condition such as temperature and ionic strength. The slope factor s and the potential dependent on the electrode system E_{const} were always monitored.

3.2.7 Potentiometric Titrations

The potentiometric titrations were all performed using a Radiometer PHM 84 pH meter and Metrohm Dosimat burette which were linked and controlled by a computer. The calibrated combined pH glass electrode of 3 M KCl internal filling solution was connected to the pH meter. During the titration, stirring was done using a Teflon magnetic stirrer bar wh le reaction solution was protected from intrusion of atmospheric oxygen and carbon dioxide by passing a continuous stream of pure nitrogen over it. All solution were prepared at constant ionic strength (I = 0.15 mol/dm^3 Cl^{-1} (Na^+)) and titrations were performed at 25 ^oC.

Before experimental titrations were done, the strong acid – strong base titrations were done in order to calculate the value of the response intercept, E^o and the value of dissociation constant of water, pK_w. These titrations were also done to check the carbonate contamination in the base stock solution. The Gran plots were made to check carbonate contamination and the contamination was shown by curvature in the region of equivalence point. The two Gran functions used are given as;[19,20,21]

$$\phi = (V_i) \times 10^{-pH} \quad ..3.38$$

$$\phi' = (V_o + V_i) \times 10^{pH} \quad ..3.39$$

where V_o is the initial reaction vessel volume and V_i is the volume of added solution at the i^{th} point of titration The pH values used in the Gran functions at each titration point were calculated using the equation;

$$pH = -((E - E_o) / s) \quad ..3.40$$

3.2.8 Protonation Titrations

After having determined the values of E_o and pK_w through the acid – base titrations and calibration of the electrode, ligand protonation titrations were performed. An aliquot of the ligand solution was dispensed into the titration vessel by a piston burette. The standardized HCl solution was added to the vessel from another burette to ensure that the ligand was completely protonated. The minimum initial volume that was required to cover the electrode was made with 0.15 mol/dm^3 NaCl solution. This solution was then titrated against the standardized NaOH at temperature of 25 ^oC. The data obtained consisted of the volume of the titre (NaOH) added and the corresponding emf values of the system at each titration point.

The concentration of the ligand in the reaction solution was determined using two Gran equations 3.38 and 3.39. Plots of Gran functions against the volume of the base added showed two different graphs. The point where ϕ intersect the x-axis shows the end-point volume of the base for free acid titration while ϕ' intersects the x-axis at the end-point volumes of the base indicates the volume of the base that was used to deprotonate the ligand. Then the concentration of the ligand was calculated by dividing the concentration of the acid associated with the ligand by the number of the ionizable protons. This concentration was more or less the same as that calculated from mass used. The concentration of the ligand calculated using Gran plots was used as an input into ESTA file template.

Having determined the values of E_o and pK_w, and the concentration of the ligand through Gran calculations, these were used as input data into ESTA file template for determination of the protonation constants. The task ZBAR with plot options 1 and 2 yielded observed and calculated curves respectively. The curves did not completely overlap but optimization of the concentrations by task OBJE resulted in good agreement between the observed and calculated formation curves. The acid concentration and protonation constant values obtained as the output after the optimization were then used for Z_H plots. Several different titrations were performed at different initial concentrations

of the ligand. The data analysis was aimed at obtaining a system that converged after fewer cycles and whose standard deviations of the optimized parameters were acceptable.

3.2.9 Complexometric Titrations

The procedure for complexation was carried out the same way as that of protonation titrations but with initial varying concentrations of solutions of the metal ions. The titrations were terminated at the first visual sign of precipitation. The titration data for each of the pairs of titrations carried out at different metal to ligand ratios were analyzed separately as pairs and then altogether as a bulk data. The input data in the ESTA file included the protonation constants, the calculated concentrations of the metal, ligand and hydrogen ions, E_o, pK_w and titration data. The constants for the hydrolysis of the metal ions were included in the computation and refinement of the formation constants.[22]

For Copper(II) hydrolysis;

$Cu^{2+} + H_2O \rightleftharpoons Cu(OH)^{+} + H^{+}$; $\log K_{10\text{-}1} = -7.87$ ..3.41

$Cu^{2+} + 2H_2O \rightleftharpoons Cu(OH)_2 + 2H^{+}$; $\log K_{10\text{-}2} = -14.33$ ..3.42

$Cu^{2+} + 3H_2O \rightleftharpoons Cu(OH)_3^{-} + 3H^{+}$; $\log K_{10\text{-}3} = -27.80$ ..3.43

$Cu^{2+} + 4H_2O \rightleftharpoons Cu(OH)_4^{2-} + 4H^{+}$; $\log K_{10\text{-}4} = -39.03$ ..3.44

$2Cu^{2+} + 2H_2O \rightleftharpoons Cu_2(OH)_2^{2+} + 2H^{+}$; $\log K_{20\text{-}2} = -10.65$ ..3.45

For Zinc(II) hydrolysis;

$Zn^{2+} + H_2O \rightleftharpoons Zn(OH)^{+} + H^{+}$; $\log K_{10\text{-}1} = -9.17$ ..3.46

$Zn^{2+} + 2H_2O \rightleftharpoons Zn(OH)_2 + 2H^{+}$; $\log K_{10\text{-}2} = -17.1$ ..3.47

$Zn^{2+} + 3H_2O \rightleftharpoons Zn(OH)_3^{-} + 3H^{+}$; $\log K_{10\text{-}3} = -28.4$ ..3.48

$Zn^{2+} + 4H_2O \rightleftharpoons Zn(OH)_4^{2-} + 4H^{+}$; $\log K_{10\text{-}4} = -40.7$ ..3.49

$2Zn^{2+} + H_2O \rightleftharpoons Zn(OH)^{3+} + H^{+}$; $\log K_{20\text{-}1} = -8.9$ ..3.50

$2Zn^{2+} + 6H_2O \rightleftharpoons Zn_2(OH)_6^{2-} + 6H^{+}$; $\log K_{40\text{-}6} = -57.6$ ..3.51

For Calcium(II) hydrolysis;

$$Ca^{2+} + H_2O \rightleftharpoons Ca(OH)^{+} + H^{+}; \quad \log K_{10\text{-}1} = -12.7 \qquad ..3.52$$

The complex species and their stability constants were determined using ESTA library of computer speciation modeling programs. The task BETA was used to evaluate the initially estimated complex species and their formation constants. The output of this task was introduced into the task OBJE within ESTA2A module to give optimized values of the stability constants and the ligand concentration describing the system.

Complex formation and deprotonation functions were calculated from stability constants obtained using the tasks ZBAR and QBAR within ESTA1 module to find out if the model fitted the system. The models were approved to be correct when the observed and the calculated plots for the Z_M and Q_M overlapped.

Finally, the task SPEC within ESTA1 module was used to determine the species distribution as a function of pH for all species in the solution over the pH range of 2 to 11.

3.3 RESULTS

3.3.1 Glycine System

The protonation and stability constants for glycine equilibria were evaluated in the pH range 2-11. The overall protonation and stability constants were confirmed by the complete overlap of the calculated and the observed Z-bar and Q-bar plots. The logarithms of overall protonation and stability constants ($\log\beta_{pqr}$) of the glycine are given in Table 3.1 together with literature values.

The protonation and stability constants were determined using ESTA library of computer speciation modeling programs. Initial guesses of the species and their constants were entered into input file. When the task BETA was used, with all guessed stability constants for a more general adjustment, the output gave modified values of the stability constants. The output values were then replaced by modified guesses and were optimized together with the acid concentration using the task OBJE to give the final values of the stability constants and the acid concentration describing the system.

Table 3.1: $\log\beta_{pqr}$ of glycine system are determined at 25 °C and I = 0.15 mol dm^{-3} (Cl^-) Na^+. s.dev denotes the standard deviation in $\log\beta_{pqr}$, R_f^H is the Hamiltonian R-factor and R_{lim}^H its limit, n_T and n_P are the number of titrations and points respectively. The general formula of a complex is $M_pL_qH_r$ denoted by the stoichiometric coefficients pqr.

	p q r	log β_{pqr}	s.dev	log K	R_f^H	R_{lim}^H	n_T (n_P)	Lit.[23]
H-gly	0 1 1	9.59	0.001	9.59	0.004	0.01	2 (202)	9.60
	0 1 2	11.96	0.003	2.37				2.37
Cu-gly	1 1 0	8.11	0.007		0.002	0.01	2 (202)	8.20
	1 2 0	14.91	0.009					15.07

3.3.1.1 H-glycine protonation

The $\log\beta_{pqr}$ obtained from ESTA were entered into the input file of task Z-bar to give Z_H-bar plots in order to check if the model was correct. The experimental and theoretical curves were obtained from flags 1 and 2 respectively in the task Z-bar of ESTA1 module.

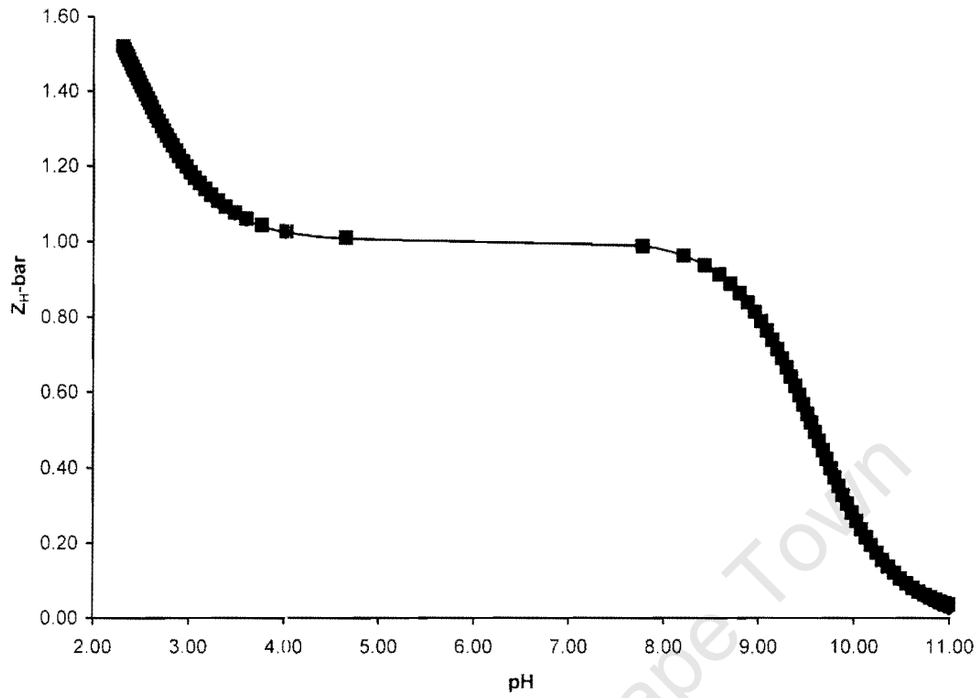

Figure 3.3(a): Protonation formation curve, Z_H-bar against pH for glycine at 25 °C in 0.15 mol dm^{-3} (Cl^-) Na^+. The symbols represent titrations performed with different starting concentrations, [(◆) 0.01 and (■) 0.008 mol dm^{-3}] and theoretical (solid line) curve.

Figure 3.3(a) shows the proton formation function, Z_H-bar plotted against pH for glycine. The Z_H-bar function rises to slightly above 1.5 for this system indicating stepwise protonation of two sites of which only one is fully protonated in the pH range studied. The two expected protonated sites are from the amino and the carbonxl groups. The experimental and theoretical curves are well superimposable thus confirming the validity of the model. The results in table 3.1 show low standard deviations and the Hamiltonian R-factor is less than its limit (R_{lim}^H) thus giving more confidence for this model.

In aqueous solutions, glycine exists as a zwitterion, the amino group being protonated ($-NH_3^+$) while the carboxyl group is deprotonated (CO_2^-).[23] The carbonxl group is protonated at pH 2-3 with $pK_{a2} = 2.37$ while the amino group with $pK_{a1} = 9.59$ is protonated at pH 8-10 as shown in figure 3.3(a). The levelling off of the curve at 1 shows the protonated amino group which begins to lose a proton in basic solution i.e. pH 8. The carbonxl deprotonation occurs at low pH where the accuracy of pH measurement is also low thus bringing about a slightly higher standard deviation than that of amino group. The pK_a values obtained are in excellent agreement with those reported in the literature.[23]

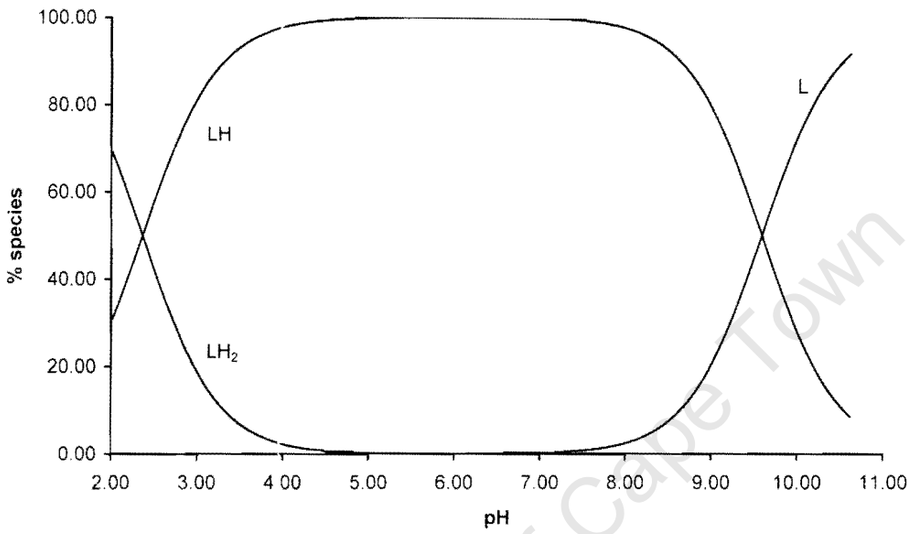

Figure 3.3(b): Protonation species distribution curves for glycine (0.01 mol dm^{-3}) as a function of pH.

Figure 3.3(b) shows the distribution of the different protonated species of glycine as a function of pH. It shows that in the pH range 4 to 7.5, all of the ligand in solution is singly protonated and that deprotonated ligand predominates above pH 7.5. The plot also indicates that the double protonation has a very short pH span. This is because the carboxyl group deprotonates at a very low pH.

3.3.1.2 Cu(II)-glycine complexation

The $\log\beta_{pqr}$ obtained from ESTA were entered into the input files of the tasks Z-bar and Q-bar of ESTA1 module to give Z_M-bar and Q-bar plots respectively. The experimental and the observed curves were obtained by flags 3 and 4 respectively for both plots.

The stability constants ($\log\beta_{pqr}$) were evaluated and confirmed by the Z-bar and Q-bar functions from the experimental data. The complex formation function, Z_M-bar, measures the average number of ligands bound per metal ion due to complexation. This function is plotted against negative logarithm of the ligand concentration (pL).

The deprotonation function, Q-bar, which indicates the average number of protons released on complexation is plotted against pH of the solution. This function is compared with n-bar function which measures the average number of protons that would be bound to the ligand in the absence of complexation.

Figure 3.3(c) shows the Z_M-bar function for the Cu(II)-glycine system plotted against pL. The levelling off of the function at a value of 2 indicates the existence of the bis complexes of 1:2 M:L ratio. The divalent copper coordinates with two molecules of glycine thus forming ML_2 species.

The Q-bar function given in figure 3.3(d) rises to two in the pH range 2.5 – 6 indicating that two proton have been released into solution due to complexation. In this pH range the glycine has only one dissociable proton (n-bar = 1) and no MLH_{-1} or an MLH_2 species is formed. ESTA analysis of the data gave the results in table 3.1. The divalent copper forms ML and ML_2 species with $\log\beta_{pq0}$'s 8.11 and 14.91 respectively. The low standard deviations illustrate the reproducibility of experimental procedure. The rising of the Q-bar to two is a result of simultaneous coordination of two molecules of the ligand glycine per copper(II) ion thus forming ML_2 species.

There is no evidence of hydroxo complex species from the above two functions curves. This is because Cu(II) forms stable species with glycine. The results are in excellent agreement with those reported in the literature.[23]

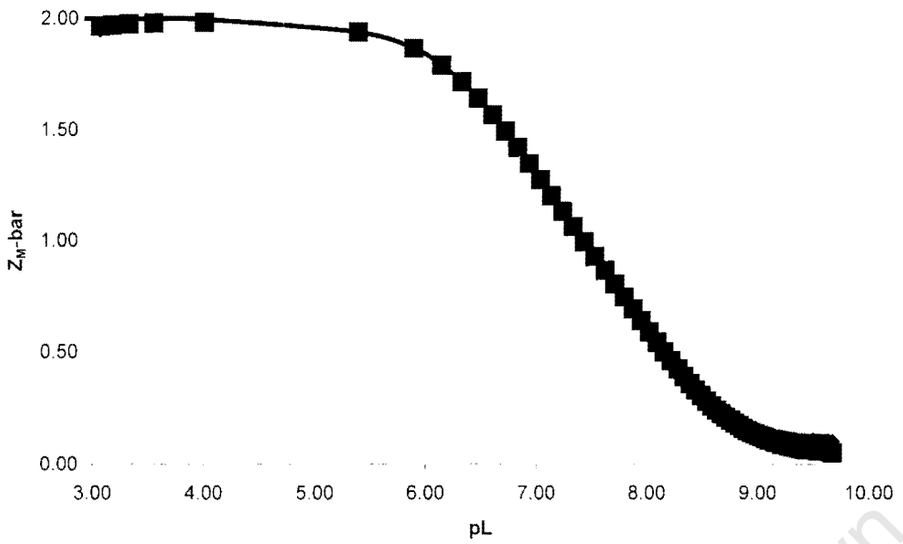

Figure 3.3(c): Formation function curve, Z_M-bar against pL for glycine at 25 °C in 0.15 mol dm^{-3} (Cl^-) Na^+. The symbols represent complexation curves for various metal to ligand ratios, [(◆) 1 : 2 and (■) 1 : 3] and theoretical (solid line) curve.

Figure 3.3(e) shows calculated species distribution curves for the Cu(II)-glycine system as a function of pH. According to the species distribution plot, complexation starts around pH 2 forming ML species until about pH 4.5. The formation of predominant ML_2 species starts at pH 3. After pH 7 the solution contains mostly ML_2 species and this concurs with the Q-bar curve levelling at 2.

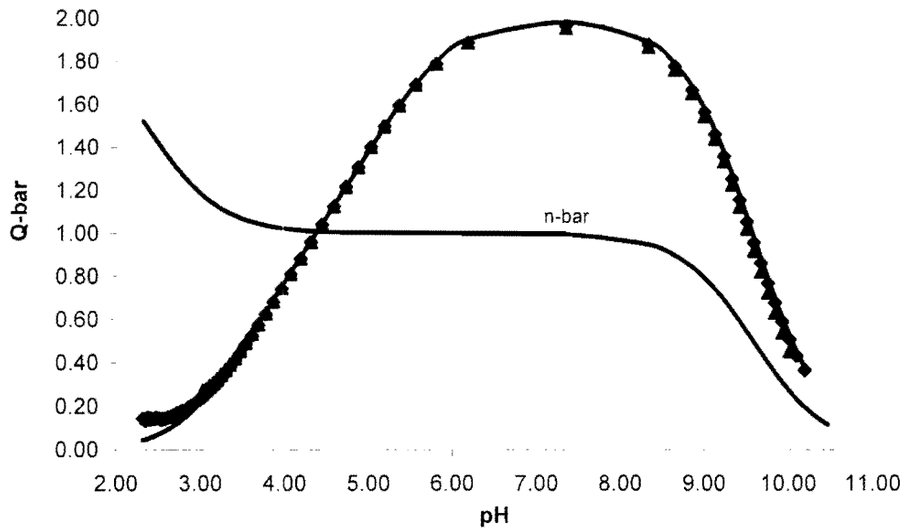

Figure 3.3(d): Deprotonation function curve, Q-bar against pH for glycine at 25 °C in 0.15 mol dm^{-3} (Cl^-) Na^+. The symbols represent complexation curves for various metal to ligand ratios, [(◆) 1 : 2 and (■) 1 : 3] and theoretical (solid line) curve.

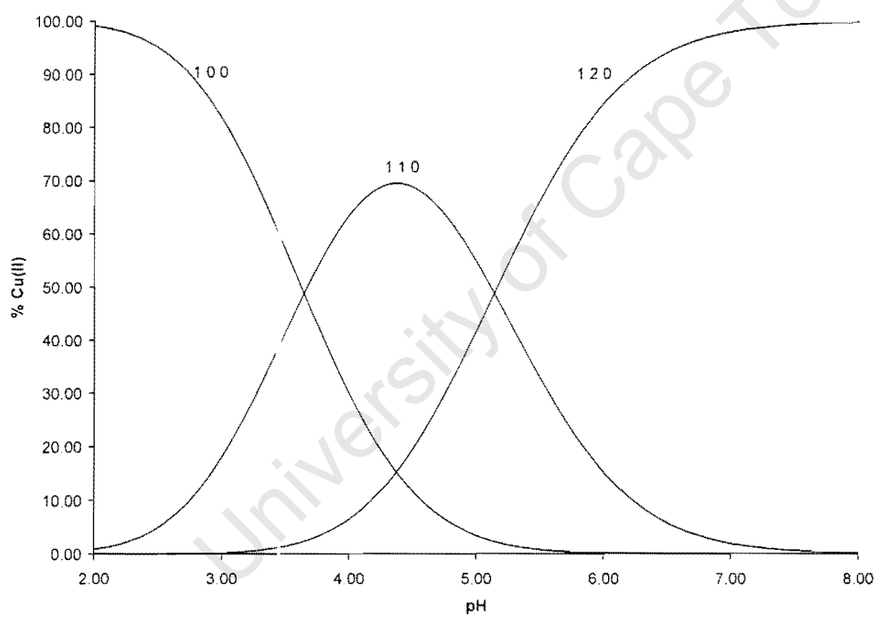

Figure 3.3(e): Species distribution curves of Cu(II) and glycine (0.0067 mol dm^{-3}, 1: 1, M : L ratio) as a function of pH.

The study of glycine system was performed in order to check the experimental procedure. The results obtained for the glycine system are very good and are in excellent agreement with the literature.[23] Therefore, this gives us more confidence in studying a new system.

3.3.2 PCUA System

The experimental procedure perfomed for the determination of protonation and stability constants for PCUA system is same as that of the glycine system. Potentiometric data was entered into ESTA l brary of computer speciation modeling programs for analysis.

3.3.2.1 Protonation

The protonation constants for H-PCUA equilibria were evaluated in the pH range 2-11. The overall protonation constants were confirmed by the complete overlap of the calculated and the observed Z_H-bar plots. The logarithms of overall protonation constants ($\log\beta_{01r}$) of the ligands are given in Table 3.2.

Table 3.2: $\log\beta_{01r}$ of PCUA determined at 25 °C and I = 0.15 mol dm^{-3} (Cl^-) Na^+. s.dev denotes the standard deviation in $\log\beta_{01r}$, R_f^H is the Hamiltonian R-factor and R_{lim}^H its limit, n_T and n_P are the number of titrations and points respectively. The general formula of a complex is $M_pL_qH_r$ denoted by the stoichiometric coefficients pqr.

Ligand	p q r	$\log\beta_{pqr}$	s.dev	log K	R_f^H	R_{lim}^H	n_T (n_P)
PCUA	0 1 1	9.52	0.01	9.52	0.03	0.01	2 (168)
	0 1 2	17.81	0.02	8.29			

Figure 3.4(a) shows Z_H-bar function curve of PCUA. The function levels off at 2 indicating that there are two dissociable protons from the primary amino groups in the PCUA ligand system. The overlapping of the experimental and the calculated Z_H-bar plots for different ligand concentrations and the low standard deviations of the $\log\beta_{0qr}$ confirm the validity of the proposed model. The titration curves show only one inflection

because the pKa values of these amino groups are so close and that they are titrated virtually simultaneously. The two protonation constants correspond to proton additions to the primary amines with $\log K_1 = 9.52 \pm 0.01$ and $\log K_2 = 8.29 \pm 0.02$.

The difference between the first and the second protonation constants is 1.23 log units. The closeness of the constants indicates proton additions to the two terminal primary amines. The difference in the constants is due to the addition of the proton to a molecule already containing a protonated site.

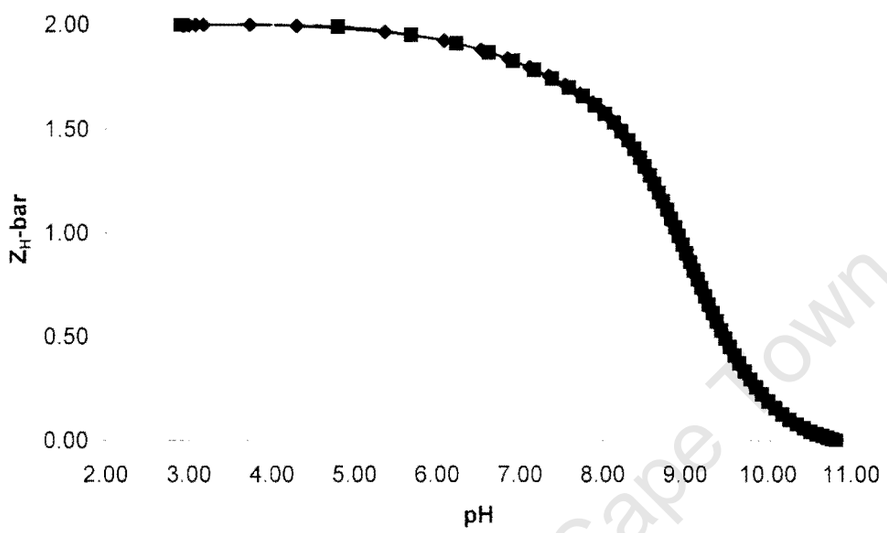

Figure 3.4(a): Protonation formation curve, Z_H-bar against pH for ligand PCUA at 25 °C in 0.15 mol dm^{-3} (Cl^-) Na^+. The symbols represent titrations performed with different starting concentrations, [(◆) 0.0012 and (■) 0.0034 mol dm^{-3}] and theoretical (solid line) curve.

Figure 3.4(b) shows calculated species distribution for PCUA. The plots indicate that deprotonation of the doubly protonated PCUA ligand begins around pH 5.5 and neutral form of the ligand predominates in the basic pH region. It is also reflected in the protonation formation curve that the deprotonation of the ligand begins around pH 5.5.

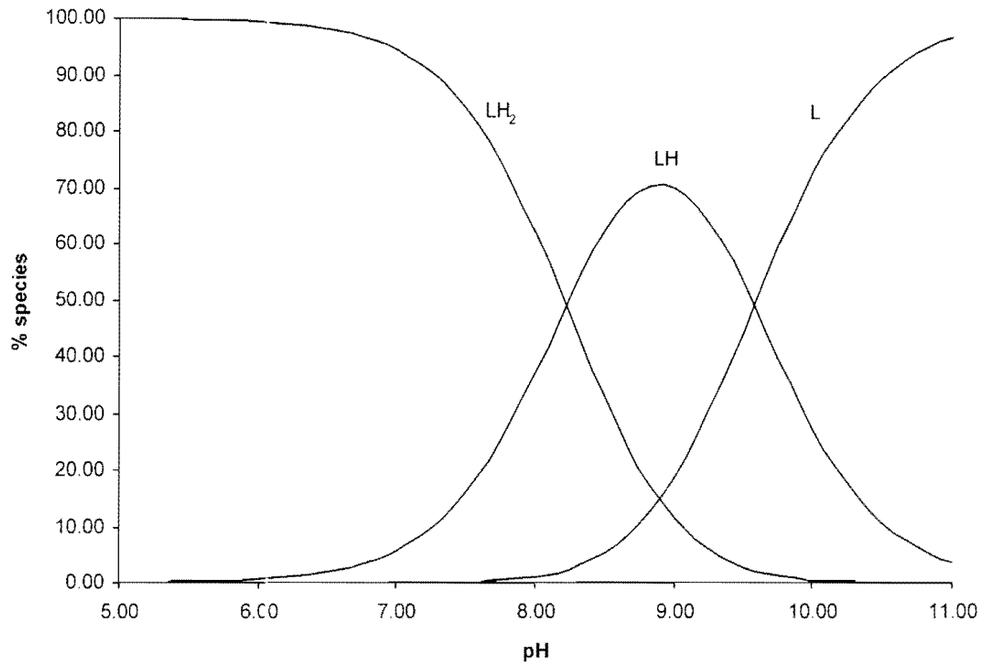

Figure 3.4(b): Protonation species distribution curves for ligand PCUA (0.0034 mol dm^{-3}) as a function of pH.

3.3.2.2 Complex formation and deprotonation functions

The stability constants ($\log\beta_{pqr}$) were evaluated and confirmed by the Z-bar and Q-bar functions from the experimental data. The complex formation function, Z_M-bar, measures the average number of ligands bound per metal ion due to complexation. This function is plotted against negative logarithm of the ligand concentration (pL).

The deprotonation function, Q-bar, which indicates the average number of protons released on complexation is plotted against pH of the solution. This function is compared with n-bar function which measures the average number of protons that would be bound to the ligand in the absence of complexation.

3.3.2.3 Complexation with Copper(II)

Table 3.3: $\log\beta_{pqr}$ of PCUA with Cu(II) determined at 25 °C and I = 0.15 mol dm^{-3} (Cl^-) Na^+. s.dev denotes the standard deviation in $\log\beta_{pqr}$, R_f^H is the Hamiltonian R-factor and R_{lim}^H its limit, n_T and n_P are the number of titrations and points respectively. The general formula of a complex is $M_pL_qH_r$ denoted by the stoichiometric coefficients pqr.

Ligand	p q r	log β_{pqr}	s.dev	R_f^H	R_{lim}^H	n_T (n_P)
PCUA	1 1 1	15.50	0.03	0.02	0.02	6 (344)
	1 1 0	9.96	0.02			
	1 1 -1	2.71	0.03			
	1 1 -2	-7.05	0.04			

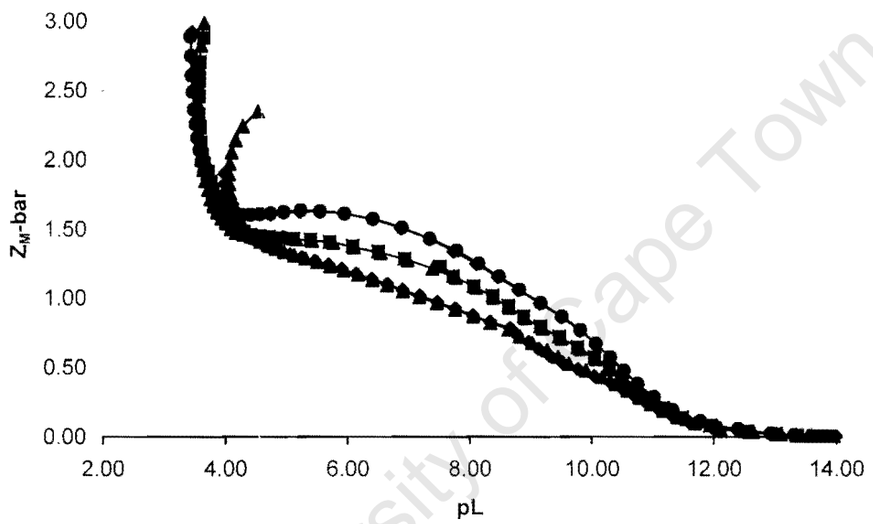

Figure 3.4(c): Formation function curve, Z_M-bar against pL for ligand PCUA with Cu(II) at 25 °C in 0.15 mol dm^{-3} (Cl^-) Na^+. The symbols represent complexation curves for various metal to ligand ratios, (▲1 : 2, ■1 : 3 and ♦1 : 4).

Figure 3.4(c) shows the Z_M-bar function for the Cu-PCUA system plotted against pL at various metal to ligand concentration ratios. The curves are non-superimposable

indicating the presence of species other than simple mononuclear species. The splitting is such that the bottom curve is for the ratio 1 : 2 and the top one for 1 : 4 metal to ligand ratio. The fanning back of the curves at pL less than 4 is indicative of the formation of hydroxo and or mixed hydroxo complexes. Those possible hydroxo species are the 1 1 -1 and 1 1 -2 as indicated in table 3.2.

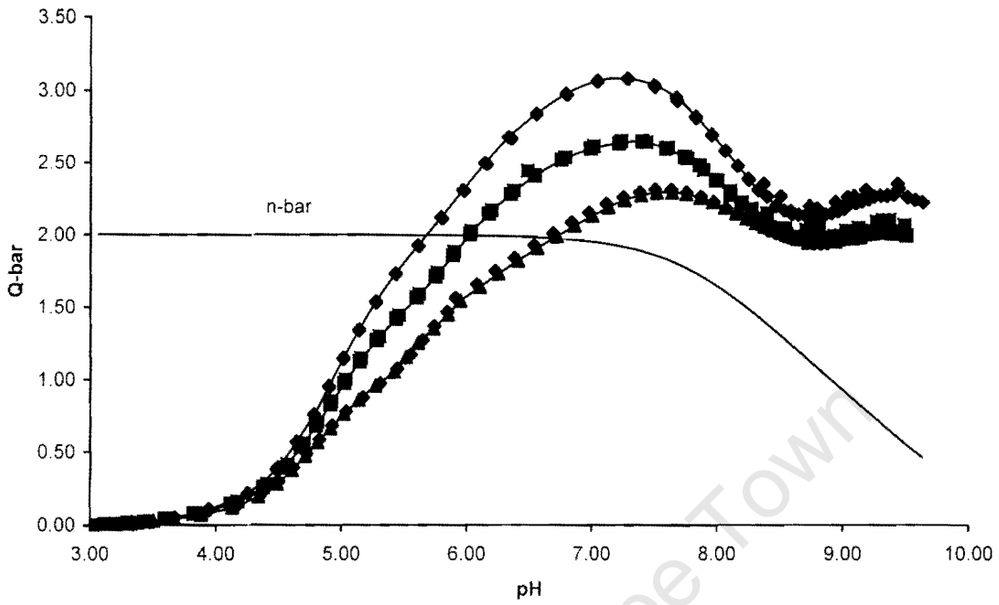

Figure 3.4(d): Deprotonation function curve, Q-bar against pH for ligand PCUA with Cu(II) at 25 °C in 0.15 mol dm^{-3} (Cl^-) Na^+. The symbols represent complexation curves for various metal to ligand ratios, (▲1 : 2, ■1 : 3 and ♦1 : 4).

Figure 3.4(d) shows deprotonation function curves as a function of pH. The Q-bar function curves indicate that deprotonation begins above a pH value of 3.5 and these curves rise above a Q-bar value of 2. The splitting pattern of the curves follows that of the formation curves. The n-bar shows that there are two possible dissociable protons on the ligand which are from the two amino groups. The rise of the deprotonation curves above Q-bar value of 2 is again an indication of hydroxo and or mixed hydroxo species. The falling of the curves at about pH 7.5 shows that complexation is complete. The rising of the curves at about pH 9 after levelling off at Q-bar = 2 is due the formation of

hydroxo species 1 1 -2. The presence of many different species was tested for using the BETA option in ESTA and using simulated data but the divergence of the curves at different M:L ratios could not be adequately explained.

The results given in table 3.3 shows logβ's with low standard deviations and an acceptably low Hamiltonian R-factor. In addition, $R^H \approx$ Rlim so it is not satistically possible to improve the model. Therefore, based on these results and, Q-bar and Z-bar plots, the proposed model is considered correct.

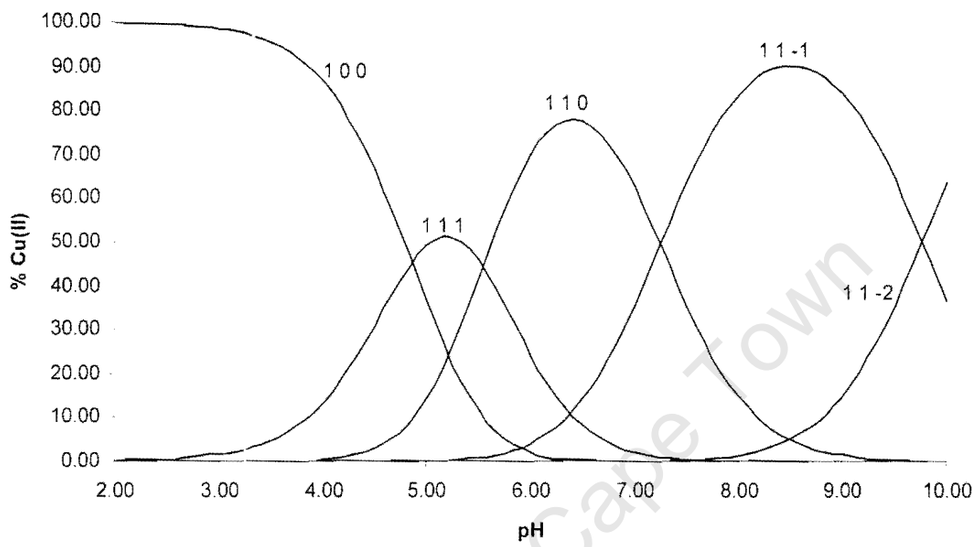

Figure 3.4(e): Species distribution curves of Cu(II) and ligand PCUA (0.0013 and 0.0033 mol dm^{-3} respectively) as a function of pH.

From the species distribution curves above, different species predominate at different regions of the pH scale. A high % Cu(II) peak is observed for 1 1 -1 species at pH 8.5 and the lowest % Cu(II) peak is observed for 1 1 1 species at pH 5.2. The Z_M-bar and Q-bar plots concur with the species distribution curves above.

3.3.2.4 Complexation with Zinc(II)

Table 3.4: $\log\beta_{pqr}$ of PCUA with Zn(II) determined at 25 °C and I = 0.15 mol dm^{-3} (Cl^-) Na^+. s.dev denotes the standard deviation in $\log\beta_{pqr}$, R_f^H is the Hamiltonian R-factor and R_{lim}^H its limit, n_T and n_P are the number of titrations and points respectively. The general formula of a complex is $M_pL_qH_r$ denoted by the stoichiometric coefficients pqr.

Ligand	p q r	log β_{pqr}	s.dev	R_f^H	R_{lim}^H	n_T (n_P)
PCUA	1 1 1	13.81	0.04	0.03	0.01	6 (519)
	1 1 0	5.55	0.03			
	1 1 -1	-2.93	0.04			
	1 1 -2	-11.74	0.03			

Table 3.4 shows four species obtained in the complexation of Zn(II) with PCUA ligand and their stability constants. The standard deviations are reasonably low and are not far from those obtained in the Cu(II)-PCUA complexation. The Hamiltonian R-factor is low thus giving confidence for the model chosen. The Z-bar function curves (figure3.5(a)) does not level off at a Z_M-bar of 1 thus indicating that the ML species are not the only species present. The curves resemble those of Cu(II)-PCUA in the splitting pattern when varying the metal to ligand ratio. The fanning back of the complex formation function at a pL of 6.5 is indicative of hydroxo and or mixed hydroxo species.

The Q-bar function (figure 3.5(b)) increases in the pH range of 4 to 7.8 followed by the steep or vertical increase from pH 7.8 indicating hydroxo species formation. This also indicates that complexation begins at about pH 4. At pH 9.5, the Q-bar and n-bar curves are parallel to each other indicating that no further complexation takes place.

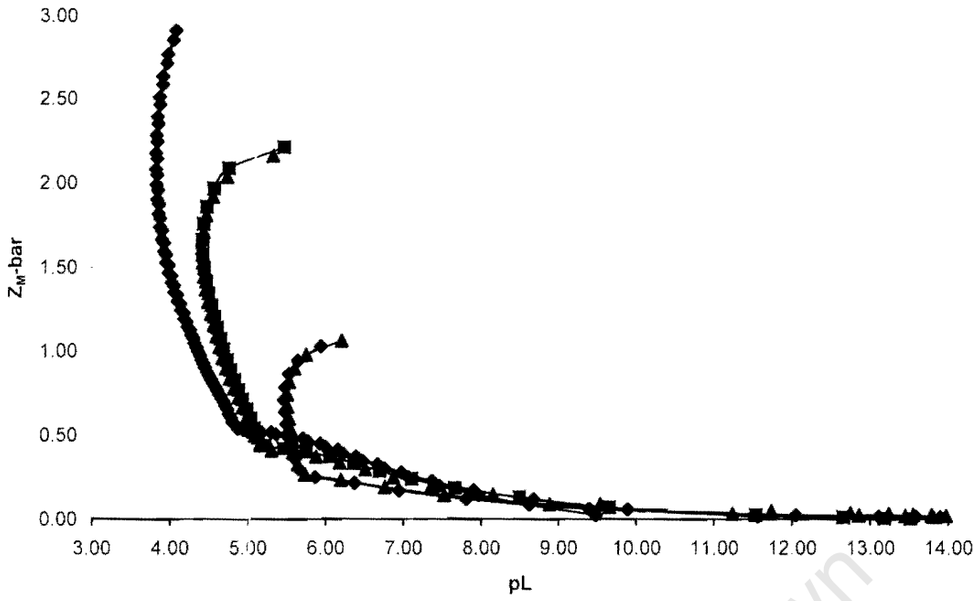

Figure 3.5(a): Formation function curve, Z_M-bar against pL for ligand PCUA with Zn(II) at 25 °C in 0.15 mol dm^{-3} (Cl^-) Na^+. The symbols represent complexation curves for various metal to ligand ratios, (▲1 : 1, ■1 : 2 and ♦1 : 3).

From the species distribution curves (figure 3.5(c)), it is evident that the protonated 111 species is present over a wide pH range. The hydroxo species formation begins at pH 7.5 and this is in agreement with the Q-bar plot. The results show that PCUA ligand is a better complexer of copper(II) as compared to zinc(II).

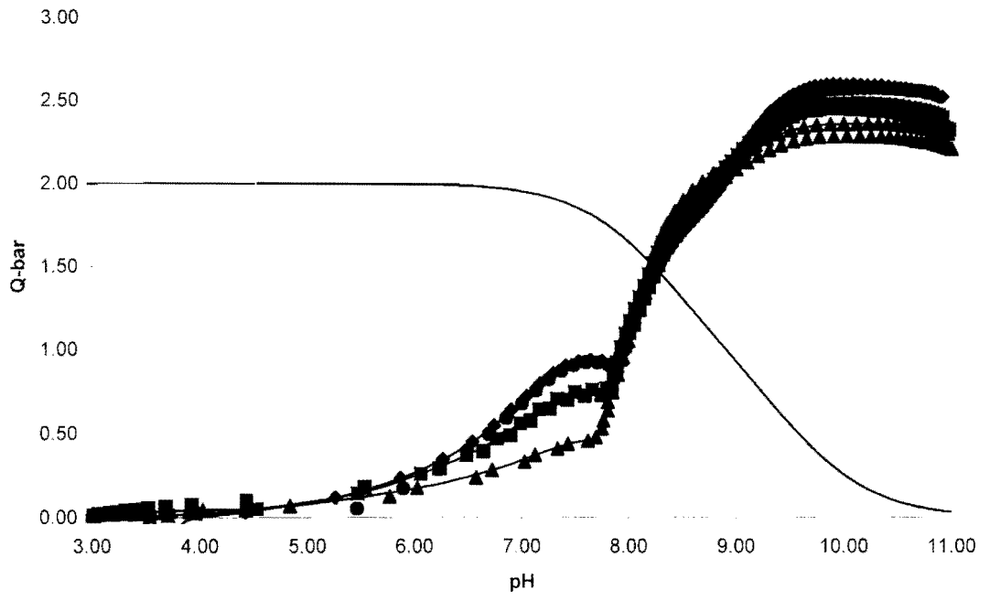

Figure 3.5(b): Deprotonation function curve, Q-bar against pH for ligand PCUA with Zn(II) at 25 °C in 0.15 mol dm^{-3} (Cl^-) Na^+. The symbols represent complexation curves for various metal to ligand ratios, (▲1 : 1, ■1 : 2 and ♦1 : 3).

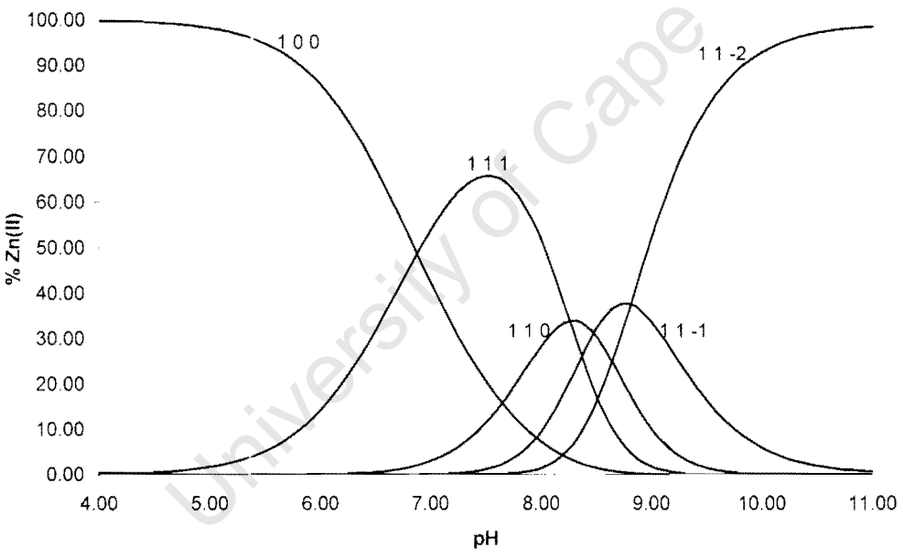

Figure 3.5(c): Species distribution curves of Zn(II) and ligand PCUA (0.00076 and 0.0017 mol dm^{-3} respectively) as a function of pH.

3.3.2.5 Complexation with Calcium(II)

Table 3.5: $\log\beta_{pqr}$ of PCUA with Ca(II) determined at 25 °C and I = 0.15 mol dm^{-3} (Cl^-) Na^+. s.dev denotes the standard deviation in $\log\beta_{pqr}$, R_f^H is the Hamiltonian R-factor and R_{lim}^H its limit, n_T and n_P are the number of titrations and points respectively. The general formula of a complex is $M_pL_qH_r$ denoted by the stoichiometric coefficients pqr.

Ligand	p q r	log β_{pqr}	s.dev	R_f^H	R_{lim}^H	n_T (n_P)
PCUA	1 1 1	13.19	0.03	0.02	0.01	6 (512)
	1 1 0	3.80	0.03			
	1 1 -1	-7.57	0.06			

The results in table 3.5 show three species formed in the complexation of Ca(II) with PCUA. It is evident from the formation function curve (figure 3.6(a)) that Ca(II) forms only weak complexes with PCUA under above conditions. The formation function curves do not increase to significant levels in the pH range investigated. The splitting pattern of the curves also resemble those of Cu(II)-PCUA and Zn(II)-PCUA systems. The deprotonation function curve (figure 3.6(b)), Q-bar remains almost constant at a value close to zero indicating that there is very poor complexation or no complexation.

However, ESTA gave stability constants reported in table 3.4. The logβ's obtained have reasonably low standard deviations and are comparable to those of copper(II) complexation. The Hamiltonian R-factor is also low thus giving confidence for proposed model.

Furthermore, the calculated species distribution curves (figure 3.6(c)) show that the protonated species (111) is present in the whole pH range investigated. There are also free Ca^{2+} ions in the whole pH range investigated indicating uncomplexed Ca^{2+} ions in the solution.

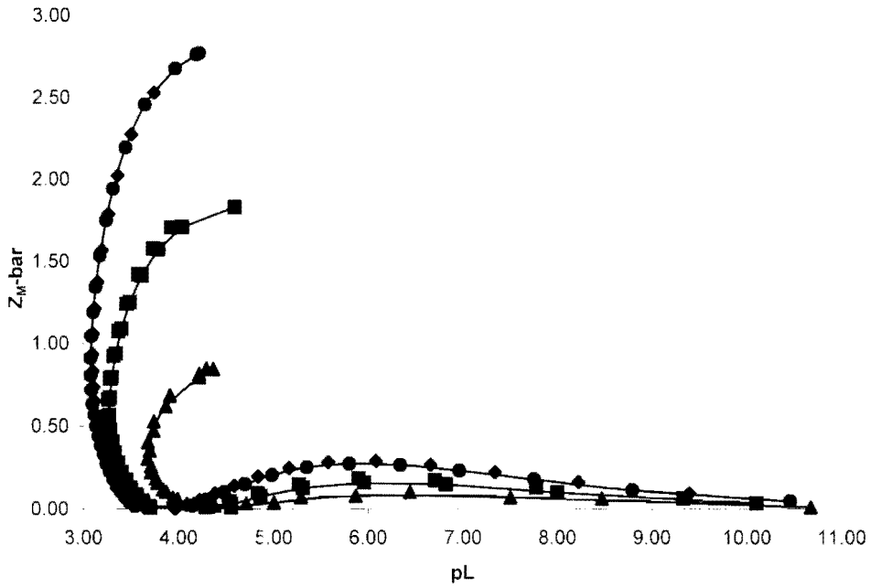

Figure 3.6(a): Formation function curve, Z_M-bar against pL for ligand PCUA with Ca(II) at 25 °C in 0.15 mol dm^{-3} (Cl^-) Na^+. The symbols represent complexation curves for various metal to ligand ratios, (▲1 : 1, ■1 : 2 and ♦1 : 3).

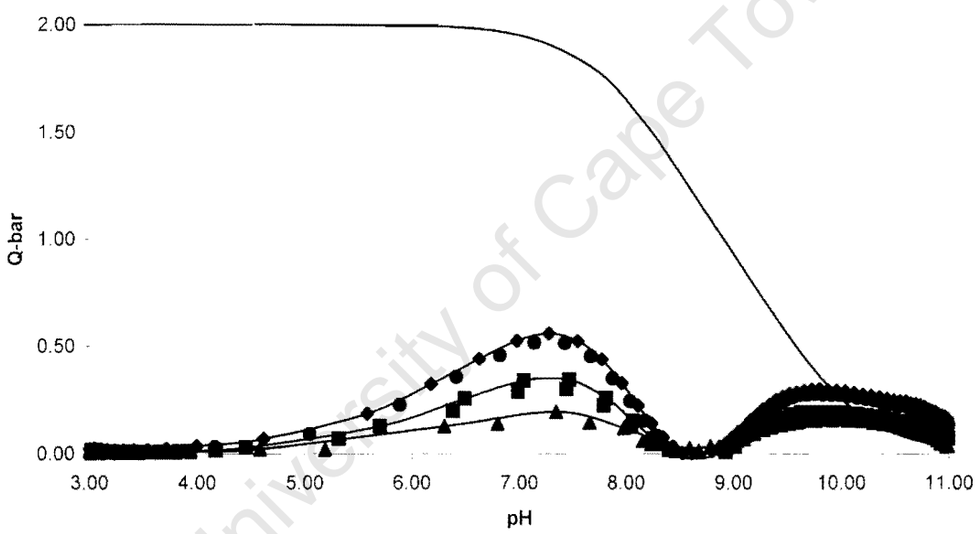

Figure 3.6(b): Deprotonation function curve, Q-bar against pH for ligand PCUA with Ca(II) at 25 °C in 0.15 mol dm^{-3} (Cl^-) Na^+. The symbols represent complexation curves for various metal to ligand ratios, (▲1 : 1, ■1 : 2 and ♦1 : 3).

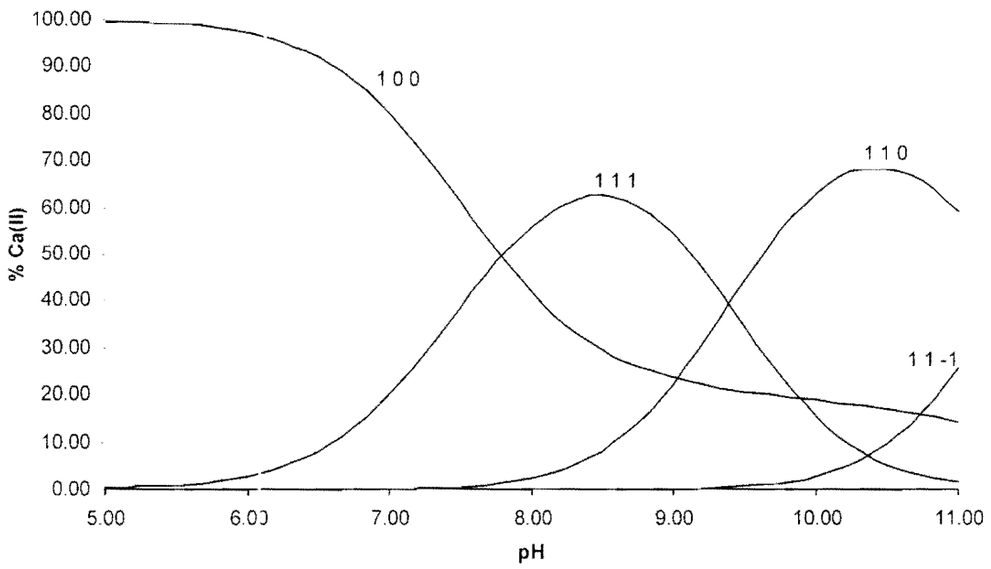

Figure 3.6(c): Species distribution curves of Ca(II) and ligand PCUA (0.00076 and 0.0017 mol dm^{-3} respectively) as a function of pH.

3.3.3 Discussion

The protonation constants of PCUA and the stability constants obtained from complexation of PCUA with copper(II), zinc(II) and calcium(II) are discussed in relation to diaminodiamide compounds (see abbreviations and structures in glossary). The proposed coordination structures of PCUA with copper(II) are given in figure 3.7 and they will be discussed in detail in chapter 4.

Table 3.6 shows protonation constants for the amino group of different diaminodiamide ligands. Protonation of the amide nitrogens was not observed. The first three ligands (5UH, 6UH and PCUA) from the table 3.6 have primary amines whereas the last two ligands(5UM and 6UM) have tertiary amines. The trend in the first protonation constant of these ligands shows an increase in the order 5UH<6UH<PCUA as the alkyl chain or group joining the two amide groups is extended. A marked increase in the basicity is observed in the order 5UM<5UH or 6UM<6UH which indicate that primary amines are

more basic than tertiary amines. The trend in the second protonation decreases in the order 5UH>6UH>PCUA.

Table 3.6: Comparison of the stepwise protonation constants of PCUA ligand with those of related diamino diamide ligands.

Ligand	Species	Log K	Medium / mol dm^{-3}
5UH	0 1 1	9.31	0.1 KNO_3, 22 °C[24,25]
	0 1 2	8.43	
6UH	0 1 1	9.40	"
	0 1 2	8.68	
PCUA	0 1 1	9.52	0.15 NaCl, 25 °C
	0 1 2	8.29	
5UM	0 1 1	8.72	0.15 NaCl, 25 °C[26]
	0 1 2	7.91	
6UM	0 1 1	8.83	"
	0 1 2	8.07	

3.3.3.1 Complexation with copper(II)

The complexation reaction of PCUA with copper(II) was evidenced by a colour change from blue to blue green. The data analysis performed using ESTA gave 1 1 1, 1 1 0, 1 1-1 and 1 1 -2 complex species with log β's 15.50, 9.96, 2.71 and -7.05 respectively.

Table 3.7: Stability constants of copper(II) with PCUA ligand and those of related diamino diamide and penta-nitrogen donating ligands.

Species	5UH[26]	6UH[26]	PCUA	EDA[29]	BIDPAP[30]
1 1 1	-	-	15.50	15.1	15.02
1 1 0	9.41	7.93	9.96	10.5	8.91
1 1 -1	7.51	6.37	2.71	2.07	-0.896
1 1 -2	8.10	6.38	-7.05	-7.3	-8.677

The proposed structures in figure 3.7 are used as a guideline for discussing the species formed. From these structures, 1 1 1 species seems to be formed by deprotonation and coordination of one of the terminal primary amines and one or both carbonyl oxygens to Cu^{2+}. It has been observed from the speciation plots that 1 1 1 species is formed at relatively low pH. There is little stabilization of this species due to the binding of the neutral carbonyl oxygen(s) to Cu^{2+}.[28]

It is expected that as the pH increases, Cu(II) would induce ionization of the amide protons. There would also be a transition from Cu-O to Cu-N in coordination arrangement.[27] The deprotonation of one of the amide nitrogens with $pK_{110} = 5.54$ ($\log\beta_{111} - \log_{110}$) results in the 1 1 0 species. This low pK is due the deprotonation of an amide from already Cu(II) coordinated ligand. The 1 1 0 species is a subsequently converted to the 1 1 -1 complex by a coordination to the other amine group with $pK_{11-1} = 7.25$ ($\log\beta_{110} - \log_{11-1}$). The 7.25 log units difference is comparable to the value of 7.8 of the overall stability constant of the second ammoniation of Cu(II) ion.[32]

The 1 1 -2 species formation is a result of loss of the second amide proton and the difference in log units from 1 1 -1 to 1 1 -2 species is 9.76 ($\log\beta_{11-1} - \log_{11-2}$). The 9.76 log units difference is associated with loss of proton from amino origin on the complex. The formation of neutral 1 1 -2 complex is observed at high pH. This species is formed when all the four nitrogens in the ligand are coordinated to the metal ion thus making 5,10,5 membered ring. It is reported that an increase in number of chelate rings around the metal ion results in large girdle strains thus influencing the stability of complexes formed.[27] It was also found that sequence 5,5,5 was less favourable as compared to the 5,6,5 or 6,5,6 membered rings.[31]

Figure 3.7: Proposed coordination structures of copper(II) with PCUA (coordinated water molecules have been omitted).

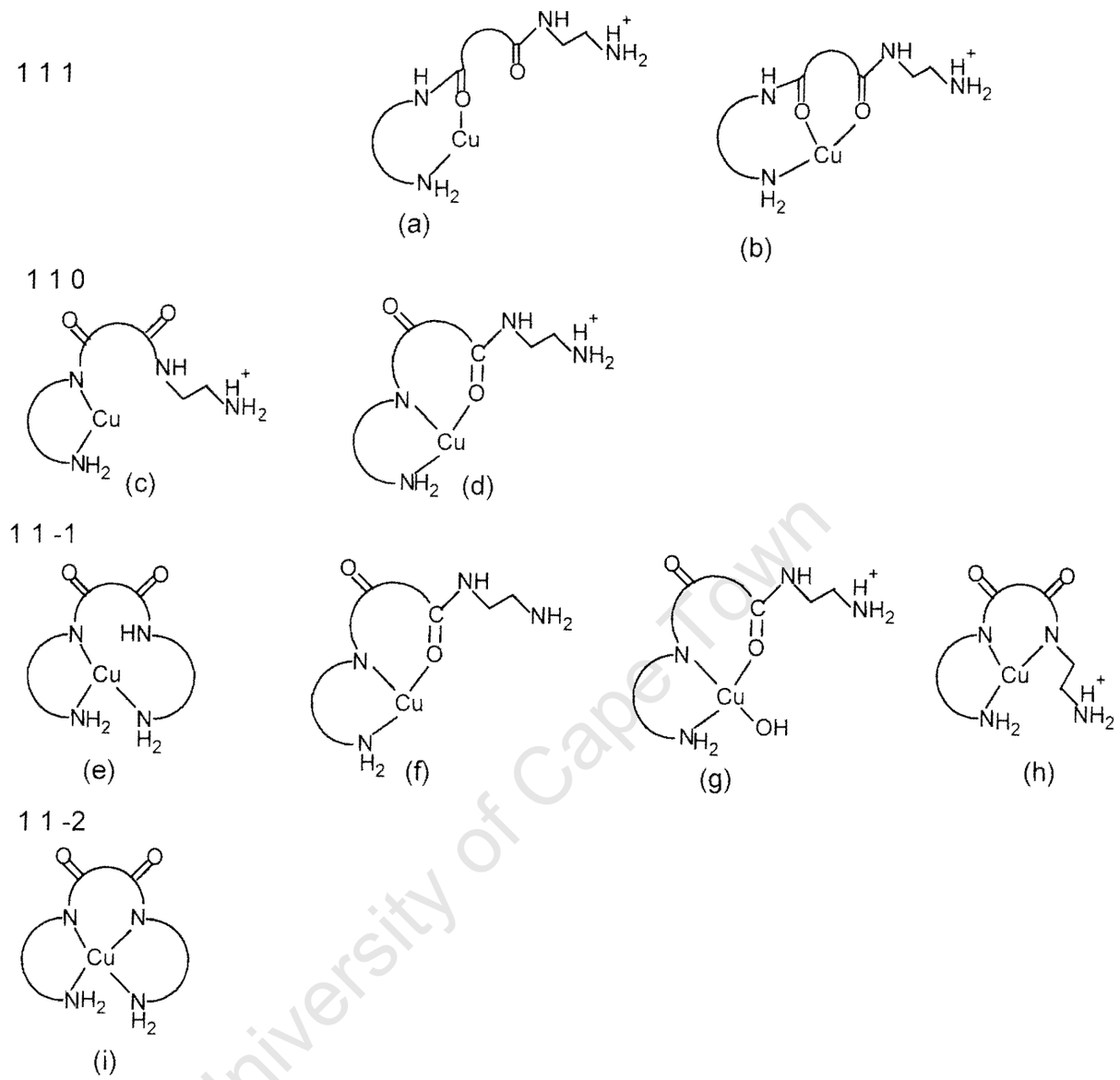

3.3.3.2 Complexation with zinc(II)

The formation curves for Zn(II)-PCUA system indicate that very little complexation occurs before the formation of an hydroxo species at pL 5.6. This is evidenced by the fanning back of the Z-bar curves. However, the chemical model shows four complex species which are 1 1 1, 1 1 0, 1 1-1 and 1 1 -2 with log β's 13.81, 5.55, -2.93 and -11.74 respectively. The complexation of zinc(II) starts at a slightly high pH (above pH 4.6) as compared to copper(II) which starts at pH 3. This is because zinc(II) is too weak an acid to promote amide deprotonation. However, the stability constants of Zn(II) complexes are also lower than those found for Cu(II). The species formation may be a result of coordination to the amine groups. Due to the electronic characteristics of the d^{10} Zn(II) ion and its large size compared to Cu(II), Zn(II) ion does not favour deprotonation of the amide nitrogen.[33] Therefore, the formation of 1 1 -1 and 1 1 -2 complexes may be due to ionization of the coordinated water molecule. Zn(II) easily form tetra-, penta- and hexa-coordination geometries. However, zinc enzymes usually have coordination numbers fewer than six so that they open reactive sites.[34]

3.3.3.3 Complexation with calcium(II)

There is very little or poor interaction between Ca(II) and PCUA ligand in solution. This is also characterized by the formation of hydroxo species and free Ca(II) ions in the whole pH range investigated(figure 3.6(c)). However, three species formed are 1 1 1, 1 1 0 and 1 1 -1 with log β's 13.19, 3.80 and -7.57 respectively. The formation of 1 1 0 species from 1 1 1 may be due to metal assisted deprotonation of the amine group with $pK_{110} = 9.39$ ($\log\beta_{111} - \log_{110}$). The observed species may also be a result of the coordination of the carbonyl oxygen and water molecules.[35]

References

1. Martel A.E., Motekaitis R.J., *Determination and Use of Stability Constants*, 1988, VCH, New York

2. Willard H.H., Merritt L.L., Dean J.A., Settle F.A., *Instrumental Methods of Analysis*, 7th ed, 1988, Wadsworth Publishing Company, Calfornia.

3. Harris D.C., *Quantitative Chemical Analysis*, 4th ed, 1995, Freeman and Company, New York.

4. Linder P.W., Torrington R.G., Williams D.R., Analysis Using Glass Electrodes, 1984, Open University Press, Milton Keynes.

5. Hughes M.N., *The Inorganic Chemistry of Biological Processes*, 1972, John Wiley and Sons, London.

6. Williams D.R. (ed), *An Introduction to Bioinorganic Chemistry*, 1976, Charles C. Thomas. Publisher, USA.

7. Hartley F.R., Burgess C., Alcock R., *Solution Equilibria*, 1980, 33-144.

8. Williams D.R., *The Metals of Life*, 1971, Norstrand/Reinhold, London.

9. Rossotti F.J.C., Rossotti H., *The Determination of Stability Constants, and other Equilibrium Constants in Solution*, 1961, McGraw-Hill Book Company, Inc., New York.

10. Eisenman G., *Glass Electrodes for Hydrogen and other Cations, Principles and Practice*, 1967, Marcel Dekker, Inc., New York.

11. Beck M.T., Nagypal I., *Chemistry of Complex Equilibria*, 1990, Ellis Horwood Ltd, Chichester.

12. May P.M., Murray K., Williams D.R., *Talanta*, 1985, **32**, no6, 483-489.

13. Jackson G.E., Kelly M. J., *J. Chem. Soc. Daltan Trans.*, 1989, 2429-2433.

14. Jackson G.E., Nakani B.S., *J. Chem. Soc. Daltan Trans.*, 1996, 1373-1377.

15. Murray K., May P.M., *Equilibrium Simulation for Titration Analysis*, Version.3, 1989, UWIST, Cardiff, Wales.

16. May P.M., Murray K., Williams D.R., *Talanta*, 1988, **35**, no11, 825-830.

17. May P.M., Murray K., Williams D.R., *Talanta*, 1988, **35**, no12, 927-932.

18. Bassett J., Denny R.C., Jeffrey G.H., Mendham J. (Eds), Vogel's Textbook of *Quantitave Inorganic Analysis including Elementary Instrumental Analysis*, 1978, Longman, London.

19. Rossotti J.C., Rossotti H., *J. Chem. Education*, 1965, **42**, 375-378.

20. Gran G., *Analyst*, 1952, **77**, 661-671.

21. Gran G., *Acta Chem. Scand.*, 1950, **4**, 559-577.

22. Baes C.F., Mesmer R.E., Hydrolysis of Cations, 1976, John Wiley and Sons, New York.

23. Kiss T., Sovago I., Gergely A., Pure and Applied Chem., 1991, **63**, 597.

24. Griesser R., Fallab S., *Chimia*, 1968, **22**, no2, 90-92.

25. Martell A.E., Smith R.M., *Critical Stability Constants*, vol 2, 1975, Plenum Press, New York and London.

26. Voye A. *PhD Thesis*, University of Cape Town, 1993.

27. Chung-Sun C., Liu Si-Han., *Polyhedron*, 1984, **3**, no5, 559-566.

28. Kloleif S., Anderegg G., *Inorg. Chim. Acta*, 1997, **257**, no2, 225-230.

29. Gama-M L., *PhD Thesis*, University of Cape Town, 1999.

30. Nomkoko E.T., *PhD Thesis*, University of Cape Town, 2002.

31. Jackson G.E., Linder P.W., Voye A., *Polyhedron*, 1991, **10**, no8, 883-884.

32. Martell A.E., Smith R.M., *Critical Stability Constants*, vol 4, 1976, Plenum Press, New York and London.

33. Santos M.A., Gaspar M., Amorin M.T., *Inorg. Chim. Acta*, 1999, **284**, 20-29.

34. Kimura E., *Tetrahedron*, 1992, **48**, 6175-6217.

35. Katz A.K., Glusker J.P., Beebe S.A., Bock C.W., *J. Am. Chem. Soc.*, 1996, **118**, 5752-5763.

36. Vacca A., Sabatini A., Gristina M.A., *Coord. Chem. Rev.* 1972, **8**, 45-53.

CHAPTER FOUR

SPECTROSCOPY AND ANCILLARY STUDIES

4. SPECTROSCOPY AND ANCILLARY STUDIES

4.1 UV - VISIBLE SPECTROSCOPY

4.1.1 Introduction

Fascinating variety of colours among transition metal complexes arise from electronic transitions between energy levels whose spacings correspond to the wavelengths available in visible light. In complexes, these transitions are frequently referred to as *d-d* transitions because they involve molecular orbitals that are mainly metal *d* in character. Since this spacing depends on factors such as geometry of the complex, the nature of the ligands present, and the oxidation state of the central metal atom, electronic spectra of complexes can provide valuable information related to bonding and structure.[1] As a result, UV-visible spectrophotometry is used as a supplementary technique to glass electrode potentiometry when ionic equilibria are investigated.

The spectrophotometry provides an additional method for comparing possible chemical models not available with potentiometry. However, because the UV/visible spectra of most complexes contain broad overlapping absorption bands, parameter correlation arises and therefore, it is not usually possible to evaluate stability constants as precisely from spectrophotometric data as compared to potentiometric data. The potentiometric data may lead to a more precise analysis of the wrong model, whereas spectrophotometric data will indicate the correct model but give a less precise analysis of it. Therefore, it is necessary to combine both spectrophotometric and potentiometric data for defining the chemical model and for evaluation of the stability constants respectively.[2]

4.1.2 Electronic Spectra of Metal Complexes

Electronic spectra from transition metal ions and complexes are observed in the visible and ultraviolet regions. The spectra arise because electrons may be promoted from one energy level to another. The absorption spectra show the particular wavelengths of light

absorbed, that is the particular amount of energy required to promote an electron from one energy level to a higher level, while emission spectra show energy emitted when the electron falls back from the excited level to a lower level.[3] The absorption is observed in bands with the energy of each band corresponding to the difference in energy between the initial and final states.

The relative intensities of absorption bands may be governed by a series of selection rules. According to Laporté rule the only allowed transitions are those with a change of parity, *gerade to ungerade* ($g \rightarrow u$) and *ungerade to gerade* ($u \rightarrow g$) but not $g \rightarrow g$ or $u \rightarrow u$. This would mean that all d-d transitions in octahedral complexes are formally forbidden. Another rule states that transitions between states of different spin multiplicities are forbidden. For example, a d^2 configuration in an octahedral field would have three transitions that are spin allowed;

$^3T_{1g} \rightarrow {}^3T_{2g}$
$^3T_{1g} \rightarrow {}^3A_{2g}$
$^3T_{1g} \rightarrow {}^3T_{1g}$

However, there are mechanisms by which selection rules can be relaxed so that transitions can occur, even if only at low intensities. The bonds in transition metal complexes are not rigid but undergo vibrations that temporarily change the symmetry of the molecule. Therefore, *d-d* transitions of octahedral complexes result in low-intensity spectra. Tetrahedral complexes often absorb more strongly than octahedral complexes of the same oxidation state. The spin selection rule breaks down somewhat in complexes that exhibit spin-orbit coupling. This results in bands associated with formally spin forbidden transitions gaining enough intensity to be observed. The spin-orbit coupling and Jahn-Teller distortions often lead to more complex spectra than predicted with spin selection rule.[1,3,4,5]

4.1.3 Electronic Spectra of Copper Complexes

Many inorganic complexes including the copper complexes absorb in the visible region (400 – 700 nm). The chemistry of the copper(II) ion differs from that of the copper(I) ion in that while the latter has a closed shell configuration $(Ar)d^{10}$ and forms diamagnetic and colourless complexes, the former has an incomplete d shell configuration $(Ar)d^{9}$ and its complexes are predominantly paramagnetic and highly coloured.[6] The aqueous chemistry of copper is largely devoted to copper(II) compounds because copper(I) compounds are quite unstable in aqueous solution. Although Cu^{2+} can be dealt with as the equivalent of a one-electron case, the detailed interpretation of its spectra and magnetic properties can be somewhat complicated. However, copper(II) compounds show a single broad poorly resolved absorption band in the visible region.

Copper(II) complexes are generally blue due to absorption in the 540 – 800 nm region of the spectra. $CuSO_4{\cdot}5H_2O$ and many copper(II) salts are blue. The addition of NaOH to a solution containing Cu^{2+} gives a blue precipitate of the hydroxide. The hydrated ion $[Cu(H_2O)_6]^{2+}$ is formed when hydroxide or carbonate are dissolved in acid or when $CuSO_4$ or $Cu(NO_3)_2$ are dissolved in water. The ion has the characteristic blue colour associated with copper salts, and has a distorted octahedral shape. There are two long bonds trans to each other and four short bonds. This is called tetragonal distortion and is a consequence of the d^9 configuration.[1,3,4,5]

Most copper(II) complexes and compounds have distorted octahedral structure. These compounds absorb in the region 11,000 – 16,000 cm^{-1} and show broad absorption band. However, octahedral complexes of copper(II) are appreciably distorted due to Jahn-Teller effect and so there is more than one peak. These peaks overlap forming broad and unsymmetrical band. The octahedral arrangement causes crystal field splitting of the d orbitals on copper into lower energy e_g and high energy t_{2g} levels. The nine d electrons are arranged $(e_g)^6$ and $(t_{2g})^3$. Since t_{2g} level is not symmetrically filled, Jahn-Teller distortion occurs. Thus the complex is distorted.[3]

Aqueous Cu^{2+} solution form many complexes with ammonia and ammines such as $[Cu(H_2O)_5NH_3]^{2+}$, $[Cu(H_2O)_4(NH_3)_2]^{2+}$, $Cu(H_2O)_3(NH_3)_3]^{2+}$ and $Cu(H_2O)_2(NH_3)_4]^{2+}$. It is difficult to add a fifth or sixth NH_3, though it is possible to make $[Cu(NH_3)_6]^{2+}$ using liquid ammonia as a solvent. The value of Δ_o (difference in energy between orbitals) for the hexammine copper(II) ion is found in the range 10,200 – 10,700 cm^{-1}. The ligand strengths of amines towards copper(II) are in the order $NH_3 > RNH_2 > R_2NH > R_3N$. In aqueous solution Cu^{2+} ion has absorption and magnetic spectra which can be interpreted in terms of tetragonally distorted $[Cu(H_2O)_6]^{2+}$ ion, the value of Δ_o being 12,500 cm^{-1}.[7] The ligand field strength of water compared to other donors is shown by the order $Cl < H_2O <$ pyridine $< NH_3 <$ 1,2-diaminoethane.

Several complexes of copper(II) with polydentate ligands containing nitrogen have been studied and the type of complex formed by copper(II) with these ligands depends on both the number of the donor atoms and the steric requirements of the ligand molecule.[7] Copper(II) peptide complexes have been studied as models for copper(II) – protein interactions. It was observed that strong copper(II) – N(peptide) bonds are formed when protons are ionized from peptide nitrogen atoms. Other biological important donor atoms such as N(amino), N(imidazole), O(carboxylate), O(peptide), H_2O and OH^- were studied.[8]

Billo proposed a method for the calculation of total electronic transition energy contribution made by the donor atoms in the coordination sphere of the metal ion.[8] This is calculated by the formula;

$$\nu_{calc} = \Sigma \nu_i \qquad ..4.1$$

where ν_i ($x10^3$ cm^{-1}) is the energy contribution by atom i.

From the above equation the contributions of each peptide and amino nitrogens to the ν_{calc} are $(4.85 \pm 0.04)x10^3$ cm^{-1} and (4.53 ± 0.07) $x10^3$ cm^{-1} respectively while that of

carbonyl oxygen, H_2O and OH^- is (3.01 ± 0.03) x10^3 cm^{-1}each and finally (3.42 ± 0.10) x10^3 cm^{-1} by carboxylate oxygen.[8] A value of 3.38 x10^3 cm^{-1} was reported for oxime nitrogen [$Cu(H_2dmg)Cl_2$] (H_2dmg = dimethyloxime, λ_{max} = 770nm). The effects of the rest of the atoms of the ligand molecule are assumed to be either negligible or additive onto the direct effect of the coordinating atom *via* the molecular framework.

The nature of electronic transitions that are brought about by chelating ligand can be inferred from the general observation of the effect of monodentate ligands on the ligand field parameter. Table 4.1 shows the guideline that is normally used for the estimation of the ligand field imposed by nitrogen-based chelating ligands. This is also relevant to the present study.

Table 4.1: Absorption maxima of the copper(II) ammine complexes of the general formula $[Cu(NH_3)_n(H_2O)_{6-n}]^{2+}$ (Ref. 10)

n	Absorption maximum (nm)
0	790
1	745
2	680
3	645
4	590

4.1.4 Data Analysis

A solution of metal ion and ligands will normally contain a number of different species at different concentrations. These species will contribute to the absorption spectrum and thus the final spectrum will be the sum of all the species present. It is therefore difficult to obtain the spectrum of a single species.

The Beer-Lambert-Bouger law, commonly called Beer's law, is the fundamental law governing the attenuation of radiation by a specific absorbing species in spectrometry.

According to this law, the absorbance A of a solution is a linear function of the concentration of the absorbing species as given by;[2]

$$A = \log(I_o/I) = \varepsilon c l \qquad ..4.2$$

where Io and I are the intensities of the incident and emergent light beams respectively, ε is the molar absorption coefficient, c is the species concentration in mol/dm^3 and l is the optical path length.

For a given concentration and path length, the actual absorbance depends on the molar absorption coefficient of the absorbing species of interest. However, for the electronic absorption spectra of solutions containing more than one species the Beer-Lambert law can be expanded to give linear combination of terms for each individual species.

The absorbance A_{obs}, at wavelength λ and when n species are present, is given by:

$$A_{obs}^{\lambda} = \varepsilon_1^{\lambda} c_1 l + \varepsilon_2^{\lambda} c_2 l + \varepsilon_3^{\lambda} c_3 l + \ldots + \varepsilon_n^{\lambda} c_n l \qquad ..4.3$$

where ε_1^{λ}, ε_2^{λ} and ε_n^{λ} are molar absorptivition coefficients of species 1,2 and n at the same wavelength λ, and c_1, c_2 and c_n are their respective concentrations. If the path length is given in cm, ε_n^{λ} is the molar absorption coefficient of the nth species in solution at wavelength λ and has the units dm^3 mol^{-1} cm^{-1}.[9] The linear dependence of A_{obs}^{λ} on the concentrations of various species present is an important feature in the equation. If a certain species has a value of ε^{λ} equal to zero, then it does not absorb in the chosen spectral region and therefore does not influence A_{obs}^{λ}.

Complexometric titration solutions may be made up of a number of solutions of different metal and ligand concentrations, and pH. If the UV/visible spectra of these solutions are obtained at a number of wavelengths, then the spectra of the individual species can be calculated by solving a set of linear equations (equation 4.3). It is recommended that adjustment of pH of the metal-ligand complex solution be made using strong acids and

alkalis such as HCl and NaOH which do not absorb appreciably in the spectral region of interest.

Calculation of the ε can be done using a specially designed computer program that requires an input file with all the information relevant to the chemical system being studied. The information includes amongst other parameters the concentration values of each chemical species present in the reaction. These concentration values are calculated on the basis of the stability constants obtained from glass electrode potentiometry. The values of ε are then plotted against wavelength to give a spectrum showing the absorption bands of each chemical species. Since the data is analyzed independently at each wavelength the existence of a smooth spectrum is not inherent in the data analysis and so if one is obtained it lends confidence to the experiment. If the stability constants and hence the concentrations are not correct, the spectrum will be disjointed and this is indicative of a wrong chemical model. After having electronic absorption spectral information for each of the complex species the nature of the ligand field environment of the central metal ion can be determined.

A UV-spectra software program was developed in our laboratory in order to solve the expanded Beer-Lambert Law equation. The program deconvoluted the UV/visible titration data into the spectra of individual species.[24]

4.1.5 Experimental

Spectrophotometric titrations were performed for Cu(II) complexation with PCUA ligand. An aqueous solution containing 1 : 3 metal to ligand ratio was prepared and measured over the pH range 2-11. Small amounts of 0.1 mol/dm^3 NaOH and 0.01 mol/dm^3 HCl were used to adjust the pH during the titration. The solutions were kept at temperature of 25 ^{o}C.

Spectrophotometric measurements were taken automatically at 2 nm interval in the wavelength range of 340 – 820 nm using Hewlett Packard 8452A Diode Array Spectrophotometer.

4.1.6 Results

Colour changes were noticed during the titration process of Cu(II) with PCUA ligand indicating the formation of complex species in solution. It is worth noting that it was very difficult to obtain absoption sprectra at pH > 8. The spectra obtained were characterized by a lot noise or interferences and were therefore discarded. This may have resulted in missing the species forming at pH > 8. However, the absorption spectra were obtained in the pH range 3-8 as shown in figures 4.1 and 4.2.

Table 4.2: Maximum wavelengths corresponding to their molar absorption coefficients for complexes of copper(II) with PCUA in solution.

Species	ε (dm^3mol^{-1} cm^{-1})	λ_{max} (nm)
1 0 0	13.2	790
1 1 1	27.4	720
1 1 0	44.2	660
1 1 -1	95.5	590

Figure 4.1 shows electronic spectra of Cu^{2+} and PCUA in solution in the wavelength range 400-820 nm. It is observed that as the pH of the solution increases, the absorbance also increases. There is a shift in λ_{max} from high to low as the pH of the solution is increased indicating the presence of different complex species.

Figure 4.2 shows a plot of molar absorption coefficient, ε, as a function of wavelength for Cu^{2+} complex species with PCUA. The spectra show three complex species, 1 1 1, 1 1 0 and 1 1 -1. The observed broad absorption bands for these species are due to the expected $^2A_{1g} \Leftarrow {}^2B_{1g}$, $^2B_{2g} \Leftarrow {}^2B_{1g}$ and $^2E_g \Leftarrow {}^2B_{1g}$ transitions.

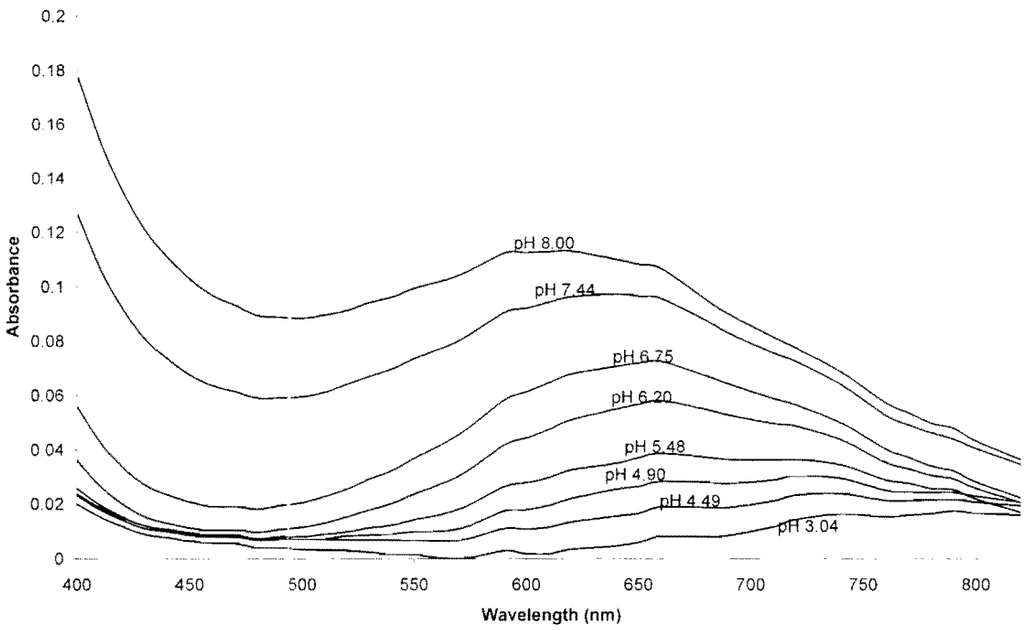

Figure 4.1: Electronic spectra of solutions containing 0.0013 mol dm^{-3} Cu^{2+} and 0.0036 mol dm^{-3} PCUA as function of wavelength.

Table 4.2 shows molar extinction coefficients and their corresponding maximum wavelengths for the three species of Cu^{2+} and PCUA. The values of ε increase in the order 1 1 1 < 1 1 0 < 1 1 -1 while the corresponding λ_{max} decrease in the order 1 1 1 > 1 1 0 > 1 1 -1.

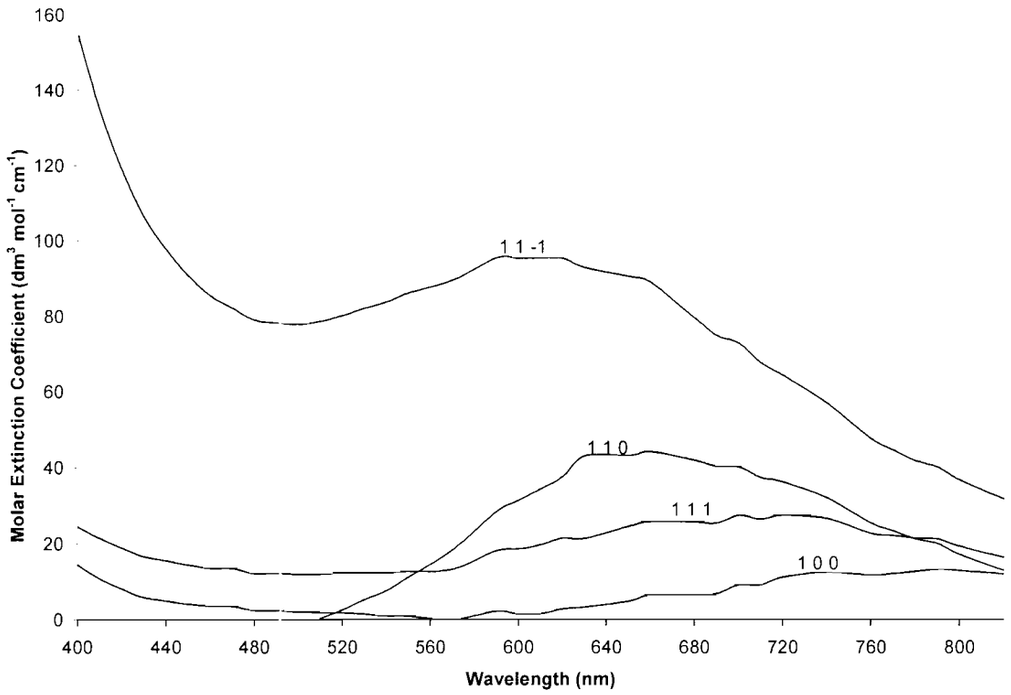

Figure 4.2: Calculated species absorption spectra of solution of Cu^{2+} and PCUA as a function of wavelength.

4.1.7 Discussion

The UV/visible spectra of the complexes of the Cu^{2+} and PCUA gave three complex species as opposed to the four species obtained from glass electrode potentiometry. The 1 1 -2 species is not observed from the UV/visible spectra because titrations were stopped at pH 8. The reason for this was that there were a lot of noise/interferences in the spectra at pH > 8. However, the spectra of the three complex species were obtained in the pH range 3-8.

The proposed structures and their details obtained using Billo's proposed method, are given in table 4.3 and figure 4.3.

Figure 4.3: Proposed structures for complexes species of Cu(II) with PCUA ligand and the corresponding calculated Billo's λ_{max}.

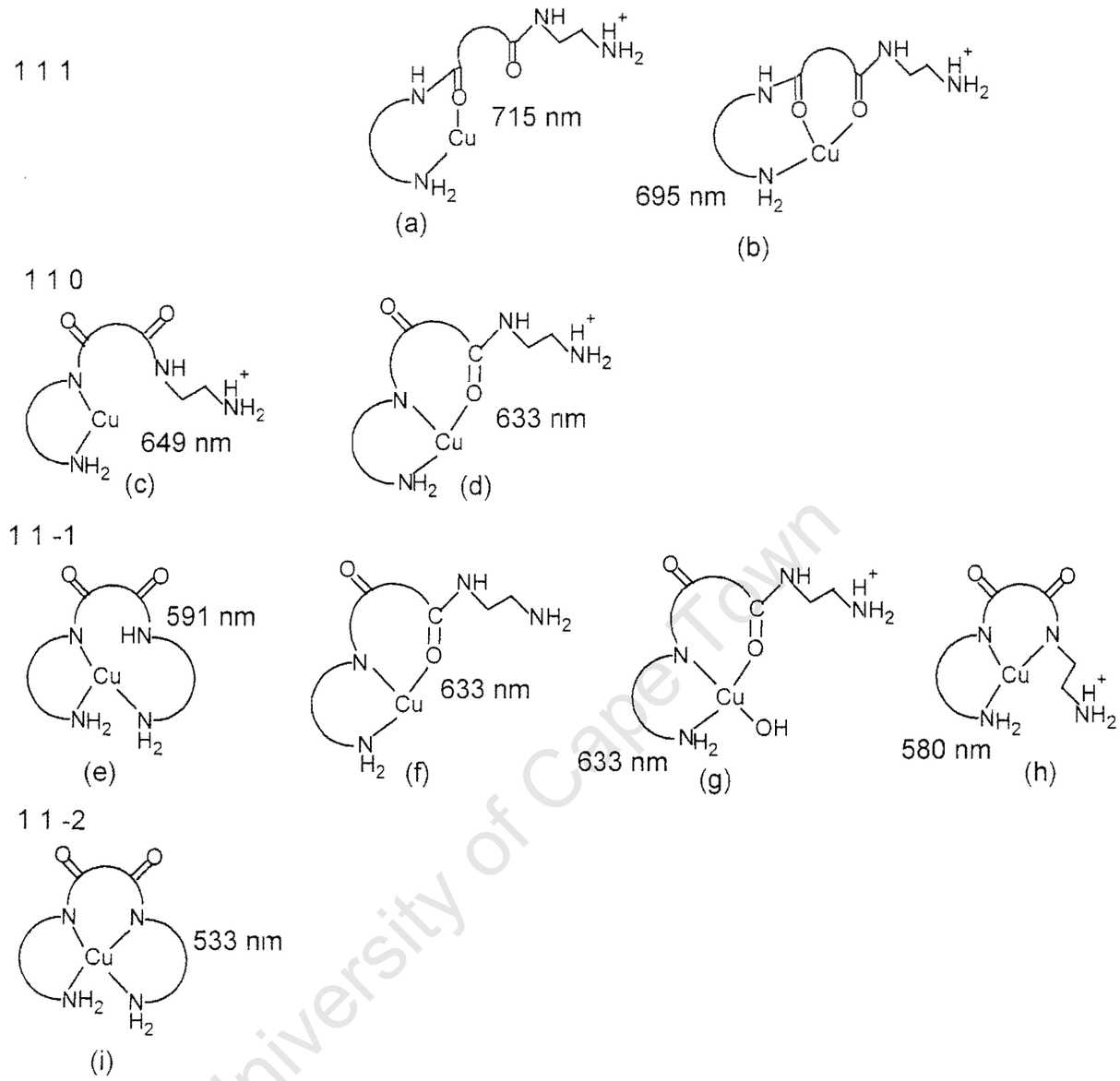

Table 4.3: Details of the proposed structures for Cu^{2+} and PCUA.

Species	Structure	$\sum \nu_{calc}$ (cm^{-1})	λ_{max} (nm)
1 1 1	(a)	13970	715
	(b)	14380	695
1 1 0	(c)	15400	649
	(d)	15810	633
1 1 -1	(e)	16920	591
	(f)	15810	633
	(g)	15810	633
	(h)	17240	580
1 1 -2	(i)	18760	533

The results given in table 4.2 for the complex species and their corresponding ε 's and λ_{max}'s, and those calculated using Billo's method in table 4.3 do concur with one another. The spectra of the complexes appear as broad spectral bands due to the nature of the 3 possible transitions.[11] The observable broad band of λ_{max} = 790 nm with low molar extinction coefficient for the 1 0 0 species is due to the uncomplexed octahedral $[Cu(OH_2)_6]^{2+}$ complex.[12]

For the MLH species in figure 4.3, structure (a) seems a more likely coordination geometry. The λ_{max} calculated from Billo's method and that obtained from the spectra are very close by 5 nm as compared to 25 nm for structure (b). The coordination geometry of the structure (b) may be destabilized by the rigidity of the cage moeity of the ligand in allowing both carbonyl oxygens coordination.

Structure (c) seems to be the best representation of the ML species. It shows coordination of the amide nitrogen that was previously uncoordinated. The reason for structure (d) having relatively low λ_{max} is due the transition of Cu-O to Cu-N when pH increases.[13] The calculated λ_{max} of 649 nm (Table 4.3) is more closer to the observed λ_{max} of 660 nm by 11 nm. Therefore, structure (c) is chosen as the best representation of 1 1 0 species.

For the MLH_{-1} species, structures (e) and (h) have close calculated λ_{max} values. The coordination geometry of structure (e) is the most likely to be formed as compared to structure (h) because the calculated λ_{max} of (e) is the same as that obtained from the spectra. The λ_{max} for (h) is 11 nm less than the calculated value. The structures (f) and (g) have λ_{max}'s same as those of the ML species, therefore, may be overlapping with ML species. However, at high pH the carbonyl oxygens are less favoured over the amino groups. This results in the deprotonation of the amino groups. Although MLH_{-2} species was not observed in the spectra, the structures (a), (c) and (e) lead to the proposed structure (i) with calculated λ_{max} of 533 nm.

The results obtained are comparable to those of $[Cu(NH_3)_n(H_2O)_{6-n}]^{2+}$ with λ_{max} for the coordination of the first, second and third amino groups given as 745 nm, 680 nm and 645 nm respectively.[10] The results are also comparable to those of diaminodiamide (5UM) (Table 4.1). The observed λ_{max} for 5UM are 675 nm and 620 nm for 1 1 0 and 11-1 respectively.[10,14]

4.2 THE BLOOD PLASMA MODEL

Metal ions play an important role in biological systems. Metal ions which are considered essential to human life include those of calcium, magnesium, manganese, iron, cobalt, copper and zinc.[15] In biological fluids, the greater percentage of metal ions is bound to proteins. Actually, only a small fraction of these is bound to low-molar-mass (l.m.w.) compounds, mainly amino acids. Free (hydrated) metal ions exist in biological fluids only at extremely low concentrations, and these concentrations cannot play a significant role in physiological processes.[16]

The metal ions which are relatively loosely bound by other types of protein, and those which are complexed by the numerous l.m.w. ligands present and the free (aquated) metal ions, are competitive with the free metal ions.[15] However, metals bound to l.m.w. compounds play a major role in many biological and physiological processes like intestinal absorption, cell absorption and renal excretion.[16] The l.m.w. complexes are believed to be involved (i) as intermediates when metal ions are inserted into or removed from certain metalloenzymes or carrier proteins, (ii) in the transfer of certain metal ions across membranes, (iii) in keeping essential metals in solution and (iv) in altering the potential of certain redox couples. Therefore, the knowledge of the equilibrium distribution of metal ions between l.m.m. ligands is highly desirable.[15,17,18]

Of interest in these l.m.m. complexes is copper. In blood plasma, 90% of the copper is irreversibly bound to ceruloplasmin, 10 % is reversibly bound to serum albumen and a small amount <1% is distributed amongst l.m.m. complexes predominantly [Cu(histidate)(cystinate)].[19] In patients with inflammatory disease, elevated levels of plasma copper are found and these levels return to normal upon remission. It is thought that the l.m.m. fraction of copper is responsible for anti-inflammatory activity, possibly by making the copper available to superoxide dismutase.[20]

The total concentrations of Mn(II), Fe(III), Cu(II), Zn(II) and Pb(II) in normal blood plasma are between 1×10^{-7} and 5×10^{-5} mol dm^{-3}.[15,17] The corresponding minute

concentrations of the respective free ions are far below the limit of detection by any analytical technique. It is also very difficult to get information from large chemical systems because of their complexity. Because of these limitations computer models simulating the complex systems have been developed.

Computer simulations of the metal-ligand equilibria in blood plasma have been performed using the general computer programs, COMICS and HALTAHALL.[21] They were both limited in respect of the way they stored data and in respect of their equation solving algorithms. They could not, therefore, treat hundreds of components and tens of thousands of complexes which might reasonably be expected to form in a complicated mixture such as blood plasma.[21]

For this reason, a specialized computer program was written in order to handle a large number of possible species. This was called ECCLES (for "Evaluation of Constituent Concentrations in Large Equilibrium Systems).[15] ECCLES solves the relevant mass balance equation and displays the resulting species distributions in ordered way to enable changes in concentrations of the major complexes to be readily monitored. One of the major features of ECCLES is its preprocessor MIX which generates estimates of the equilibrium constants for the many mixed (ternary) complexes that might be important in the blood plasma.[21] Table 4.4 contains a list of the predicted most predominant l.m.w. complexes of copper present in the blood plasma. As can be seen, most of these complexes are mixed, ternary complexes of histidine and another amino acid.

In order to understand the effect of the ligand (drug) on the equilibria present in this model, formation constants of the ligand and the species of interest determined in vitro, are incorporated into a database. This database, on inclusion of the drug concentration, is interrogated by the ECCLES computer program to yield results pertaining to the influence of this drug on these equilibria.

Table 4.4: Calculated % distribution of Cu(II) among its most predominant l.m.w. complexes in blood plasma.[22,23]

Complex species	log β	% of total l.m.m. Cu(II)
Cu-(his)(gln)	16.70	19.2
Cu-$(his)_2$	17.50	15.5
Cu-(his)(thr)	17.03	13.7
Cu-(his)(ser)	16.97	7.5
Cu-(his)(ala)	17.00	5.4
Cu-(his)(Lys)H^+	27.05	4.4
Cu-(his)(gly)	16.94	4.3
Cu-(his)(asn)	16.81	4.2
Cu-(his)(val)	16.93	3.9
Cu-(his)(leu)	17.18	3.7

Symbols: his = histidinate, gln = glutaminate, thr = threoninate, ser = serinate, ala = alaninate, lys = lysinate, gly = glycinate, asn = asparaginate. val = valinate, leu = leucinate.

One of the limitations of this program is that protein equilibria are not included and therefore the concept of plasma mobilizing index (pmi) is used. It is defined as the ratio of the total concentration of l.m.w. metal complex species in the presence of the drug to that in normal blood plasma. In simple terms, pmi is a measure of the ability of the administered ligand to move the metal ion from the protein bound fraction to the l.m.w fraction. It is based on the premise that the free concentration of the metal ion is buffered and hence held constant during any reasonable perturbation.

The l.m.w. fraction of copper(II) is postulated to be involved in the transport of the ion across the biomembranes to anti-inflammatory processes. Therefore, the study of this blood plasma model is done to measure the availability of the metal ion to the anti-inflammatory processes by l.m.w. ligand PCUA.

4.2.1 Simulation Studies

In investigating the copper specificity of the ligand of present study, the potentiometrically determined stability constants for copper(II), zinc(II) and calcium(II) complexes were put into the ECCLES model of blood plasma so as to calculate the plasma mobilizing indices. The inclusion of Zn(II) and Ca(II) is due to their high concentrations in blood plasma relative to Cu(II).[15] In the calculation, the total ligand concentration was raised over the range 10^{-2}-10^{0} mol dm^{-3}. The results are given in figures 4.5 and 4.6.

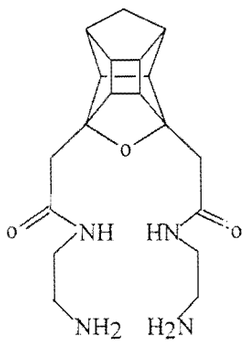

PCUA

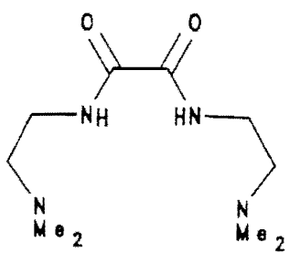

5UM

Figure 4.4: Structures of PCUA and 5UM

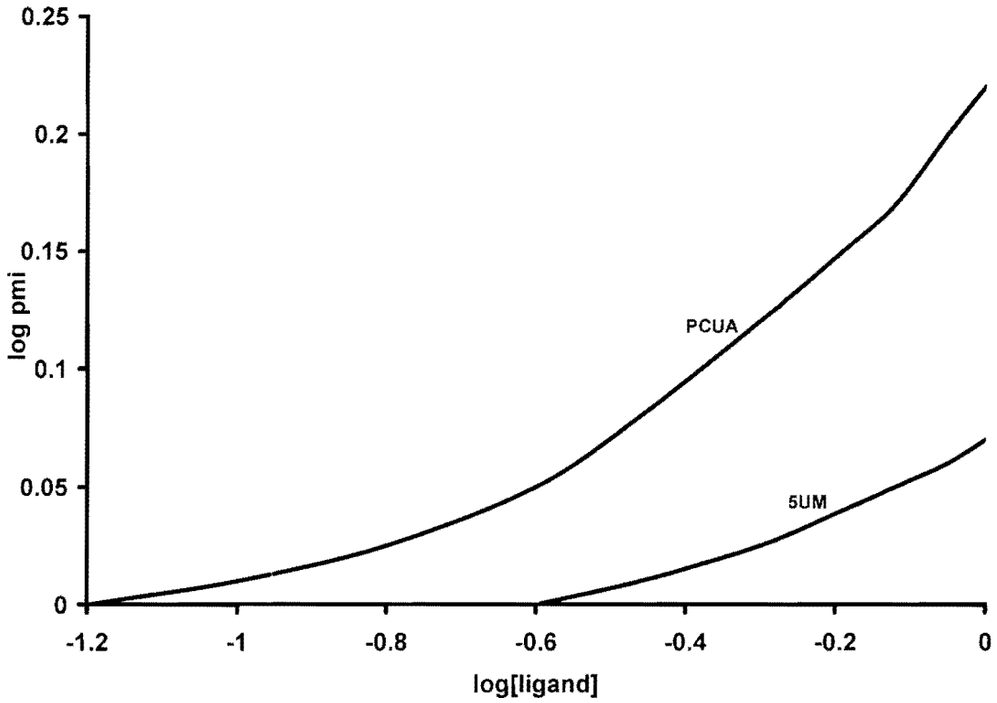

Figure 4.5: Logarithms of Cu(II) plasma mobilizing index as a function of logarithms of the ligand concentration for PCUA and 5UM ligands.

Figure 4.5 shows the pmi curves as a function of log[ligand] for the ligands PCUA and 5UM. These pmi curves indicate that the ligand PCUA is better able to mobilize copper than 5UM. However, the log pmi value of 0.22 at 1 M concentration is still unreasonable for biological systems. Therefore, it cannot effectively increase the l.m.w. copper(II) fraction. One of the reasons for this low mobilizing ability is the stability of the PCUA, Zn(II) and Ca(II) complexes. This is shown in figure 4.6. A 10^{-1} concentration of PCUA causes a 30 fold increase in the l.m.w. Ca(II), a 2 fold increase in l.m.w. Zn(II) and no change in the l.m.w. concentration of Cu(II).

Figure 4.6 shows the the pmi curves for Cu(II), Zn(II) and Ca(II) with PCUA as a function of log[PCUA]. The curves indicate that the mobilizing ability of PCUA is in the order Ca(II) > Zn(II) > Cu(II). This shows that zinc(II) and calcium(II) are competitors of copper(II) in blood plasma. This illustrates the need for simulation models and inclusion of other competing metal ions in the study. Looking at the stability of the Cu(II) complex

alone is not sufficient because as in this case the Ca(II) and Zn(II) being present in much higher concentrations are able to compete for PCUA.

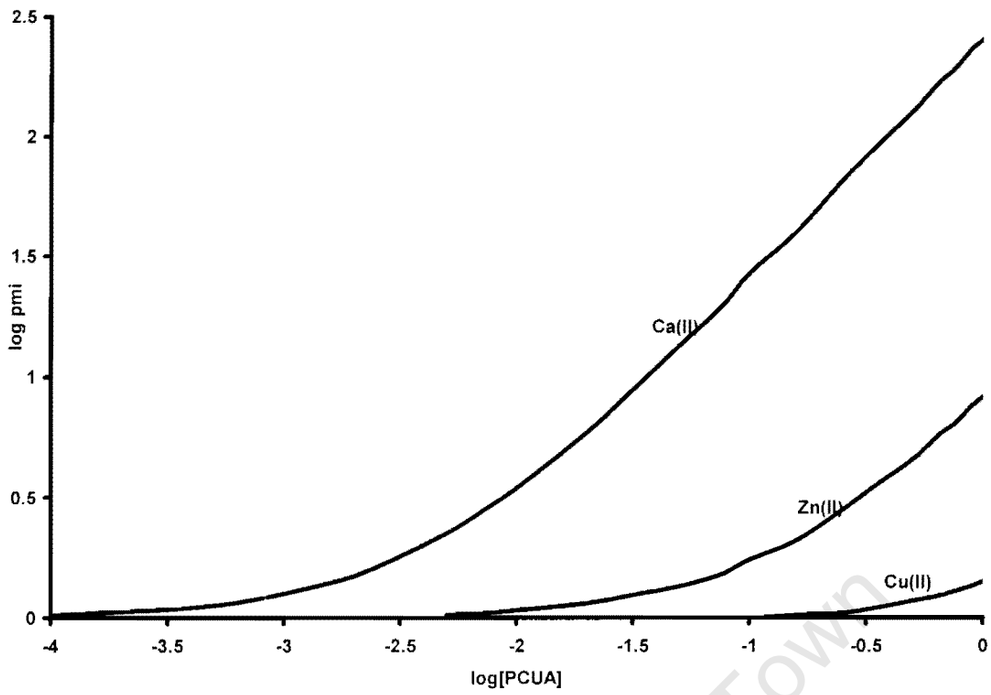

Figure 4.6: Logarithms of Cu(II), Zn(II) and Ca(II) plasma mobilizing indices as a function of log[PCUA].

4.3 NUCLEAR MAGNETIC RESONANCE

4.3.1 Introduction

Nuclear magnetic resonance (NMR) is an important tool in the investigation of chemical structures and reaction mechanisms. It has been extended to whole body imaging in medical diagnosis. In this study NMR is used to determine the sequence of protonation of the two amine groups of PCUA. The presence of the proton is expected to shift the NMR signal arising from protons attached to the neighbouring carbons. Upon complexation with copper(II), the presence of the metal is expected to broaden and shift the signal arising from protons attached to the neighbouring carbons.

3.2.2 Experimental

In 5ml glass vials. one millimetre portions of 0.015 M stock D_2O solution of PCUA ligand were prepared and the ^1H NMR spectra were recorded at 300 MHz. The pH of the solutions was adjusted using concentrated NaOH and HCl. Tertiary butyl alcohol was used as a reference. A micro-pH 2000 meter was used to measure the pH of the solutions. The pH of the solution may be calculated using the relationship;

$pD = pH + 0.4$

For copper(II)-PCUA complexation, solutions of 1:2 molar ratio of metal to ligand were prepared in D_2O and scanned in the pH range 4-11. The magnetic resonance spectra of both protonation and complexation were plotted as function of pH.

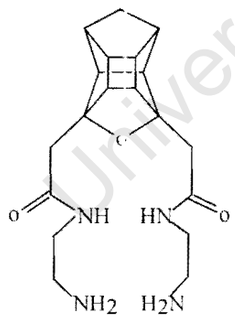

PCUA

4.3.3 Results and Discussion

Figure 4.7 shows proton NMR spectra for protonation of PCUA in D_2O. As the pH of the solution increases, some of the NMR signals shift to low ppm values. The shift is a result of protonation to the amine groups. A significant chemical shift is observed

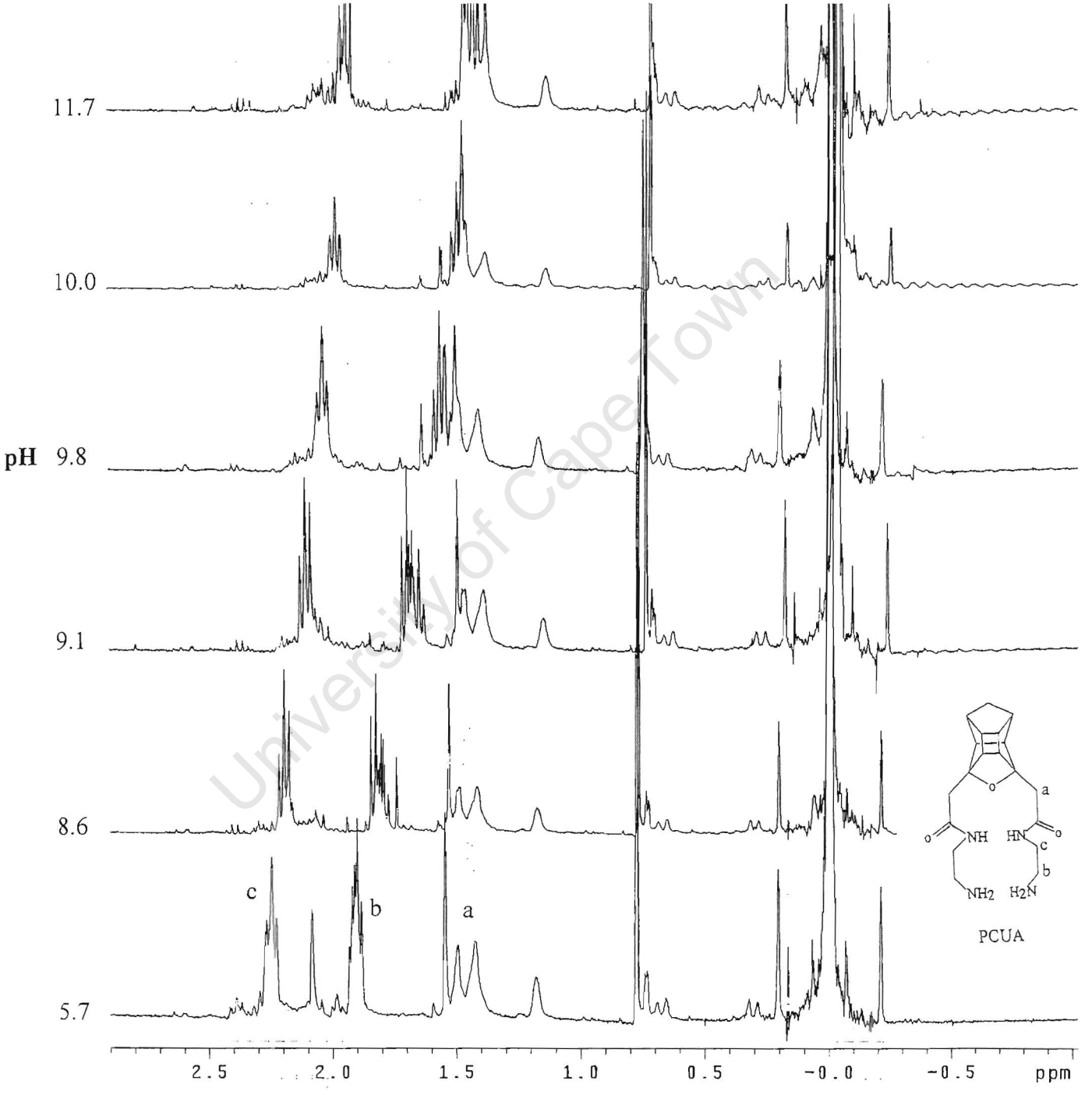

Figure 4.7: Proton NMR spectra of PCUA as a function of pH.

for protons attached to carbons next to the amine groups followed by those next to the amide groups.

Figure 4.8 shows plots of proton chemical shifts as a function of pH, where (a), (b) and (c) refer to the chemical shifts of the protons attached to carbons next to the carbonyl groups, amine groups and amide groups respectively (ligand structure given in figure 4.7). There is no significant change in the chemical shift of the (a) protons as compared to (b) and (c) protons. This is because protons at this position are far from the amine groups where protonation takes place. However, a more significant change is observed for protons (b). Other protons on the cage moiety show very slight shift or no shift because they are further away from the site of protonation.

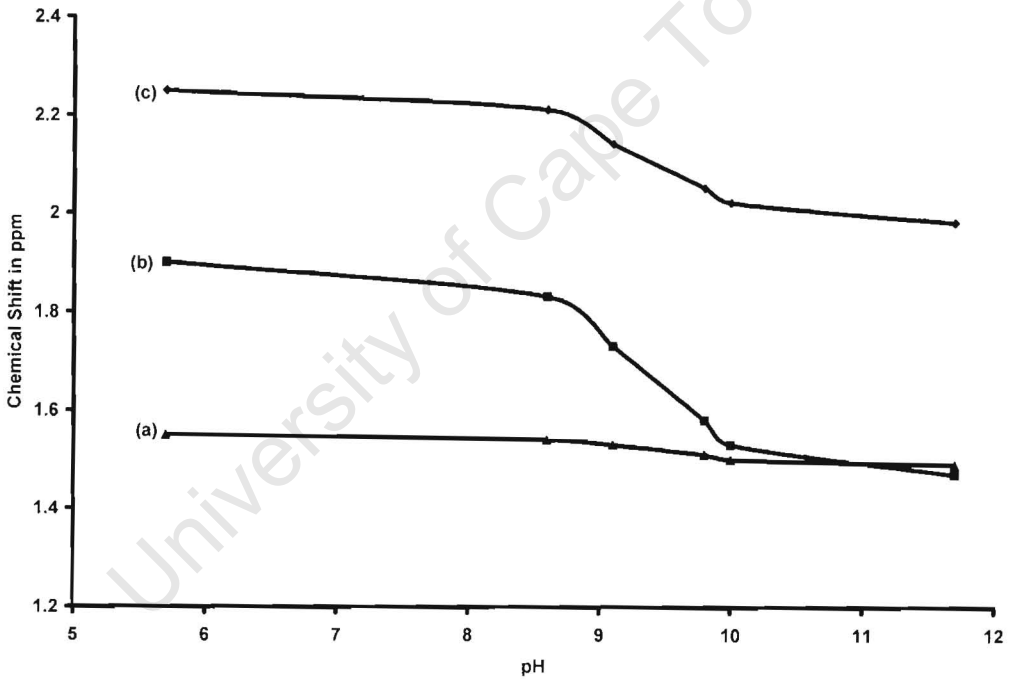

Figure 4.8: Change in proton chemical shift (ppm) as a function of pH.

The plots of change in proton chemical shift show average pKa value of 9.5 which is in good agreement with the value of 9.52 obtained from our potentiometric studies.

Figure 4.9 shows the spectra for complexation of copper(II) and PCUA as function of pH. Since copper(II) is paramagnetic, it tends to broaden and shift signals arising

from protons attached to neighbouring carbons. From the species distribution curves in figure 3.4(e), complexation of free ligand starts at pH 4 and, therefore we expect a change in the NMR spectra at pH > 4. From figure 4.9, signals (a), (b) and (c) broaden and shift as pH increases. The signal arising from protons attached to carbons next to the amine groups virtually disappear at pH 7.5 due the closeness of the Cu(II) ion. This indicates that either one or both amine groups are coordinated to the metal ion. However, the signals arising from protons attached to carbons next to the amide groups also broaden and shift to low ppm values. This is indicative of coordination of the metal ion to at least one amide group as pH increases from 4-11. The signals arising from protons which are further away from the site of coordination slightly broaden and shift to low ppm values.

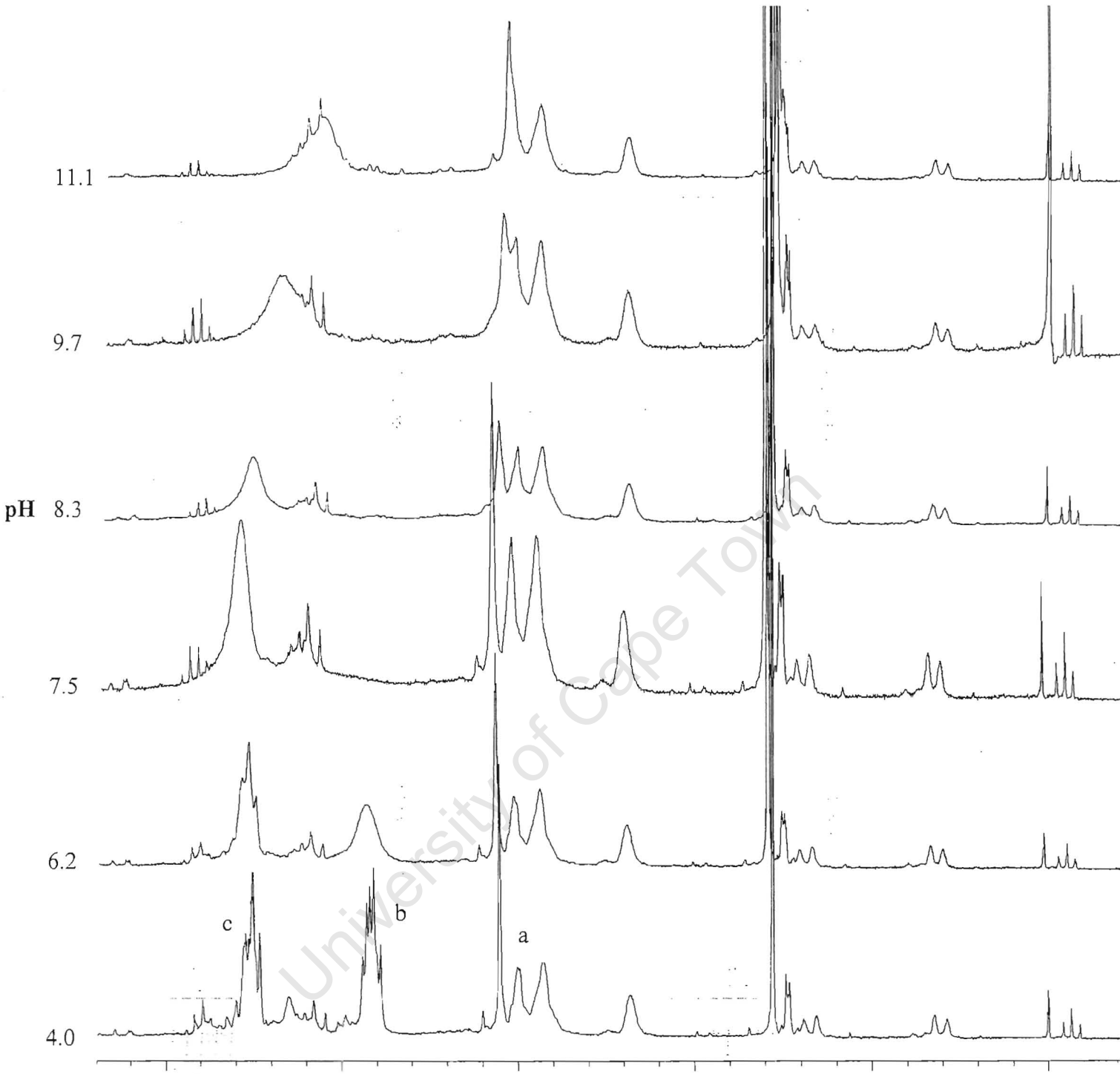

Figure 4.9: Proton NMR spectra for complexation of copper(II) with PCUA as a function of pH.

References

1. Huheey J.E., Keiter E.A., Keiter A.L., *Inorganic Chemistry, Principles of Strucrure and Reactivity*, 4th ed., 1993, Harper Collins College Publishers, New York.

2. Hartley F.R., Burgess C., Alcock R., *Solution Equilibria*, 1980, Ellis Horwood Ltd., West Sussex.

3. Lee J.D., *Concise Inorganic Chemistry*, 4th ed., Chapman and Hall, 1991, London.

4. Miessler G.L., Tarr D.A., Inorganic Chemistry, Prentice Hall, Inc., 1991, USA.

5. Cotton F.A., Wilkison G., *Advanced Inorganic Chemistry, A comprehensive Text*, 3rd ed., 1972, John and Wiley, Inc., London.

6. Wilkinson G., Gillard R.D., McCleverty J.A., *Comprehensive Coordination Chemistry*, Vol. 3, 1987, Pergamon Press, Oxford.

7. Bailar J.C., Emeleus H.J., Nyholm R., Dickenson A.F.T., *Comprehensive Inorganic Chemistry*, Vol 3, 1973, Pergamon Press, Oxford.

8. Billo E.J., *Inog. Nucl. Chem. Letters*, 1974, **10**, 613-617.

9. Jackson G.E., Nakani B.S., *J. Chem. Soc. Dalton Trans.*, 1996, 1373-1377.

10. Jackson G.E., Linder P.W., Voye A., *J. Chem. Soc. Dalton Trans.*,1996, 4605-4612.

11. Lever A.B.P., *Inorganic Electronic Spectroscopy*, 2nd ed., 1984, Elsevier, New York.

12. Kallay C., Varnagy K., Sovago I., Sanna D., Micera G., *J. Chem. Soc. Dalton Trans.*, 1998, 92.

13. Liu S-H., Chung C-S., *Polyhedron*, 1984, **3**, no5, 559-566.

14. Voye A., *PhD Thesis*, University of Cape Town, 1993.

15. May P.M., Linder P.W., Williams D.R., *J. Chem. Soc. Dalton Trans.*, 1977, 588-595.

16. Faure H., Favier A., in; *Handbook of Metal-Ligand Interactions in Biological Fluids, Bioinorganic Chemistry*, (Ed) Berthon G., Marcel Decker, Inc., New York, **2**, 1163-1169.

17. Williams D.R., *The Metals of Life*, 1971, Van Norstrand Reinhold, London.

18. Williams D.R., (Ed), *An Introduction to Bioinorganic Chemistry*, 1976, Charles C. Thomas Publisher, USA.

19. Jackson G.E., Kelly M.J., J. *Inorganic Chimica Acta*, 1988, **152**, 215-217.

20. Sorenson J.R.J., in; *Metal ions in Biological Systems, Inorganic Drugs in Deficiency and Disease*, (Ed), Sigel H., 1982, **14**, chpt.4., Mercel Decker, Inc, New York

21. May P.M., in; *Handbook of Metal-Ligand Interactions in Biological Fluids, Bioinorganic Chemistry*, (Ed) Berthon G., Marcel Decker, Inc., New York, **2**, 1184-1194.

22. Jackson G.E., in; *Handbook of Metal-Ligand Interactions in Biological Fluids, Bioinorganic Chemistry*, (Ed) Berthon G., Marcel Decker, Inc., New York, **2**, 1228-1239.

23. Brumas V., Alliey N., Berthon G., *J. Inorg. Biochem.* 1993, **52**, 287-296.

24. Jackson G.E., *UV-SPEC, Private Communication*, University of Cape Town.

CHAPTER FIVE

GENERAL DISCUSSION AND CONCLUSION

5. GENERAL DISCUSSION AND CONCLUSION

The role of copper(II) in biological systems and processes is well known.[1,2] The elevation of copper(II) complex species in the plasma and synovial fluids of rheumatoid arthritic (RA) patients is known.[2] It was also found that a number of Cu(II) chelates exhibit anti-inflammatory activity. Therefore, several studies have been carried out in designing chemically stable copper complexes for use in anti-arthritic agents.

The present study has been designed to contribute to the development of the anti-arthritic agents. However, the suitable ligand must be able to complex copper and enhance the transportation across a biomembrane. It is also required that the ligand must be able to compete with histidine for copper in plasma or form ternary complexes of histidine.[2]

This study investigated the solution equilibria of H^+, Cu^{2+}, Zn^{2+} and Ca^{2+} at 25 °C and in 0.15 mol dm^{-3} $Cl^-(Na^+)$ using glass electrode potentiometry. These metals were studied with the ligand PCUA.

PCUA has been found to take up two protons in the pH range 2-11. The observed protonation constants agree with those of related diamino diamide ligands and their analoques. From the complex formation and deprotonation functions, the stability constants reported were chosen as the best possible to describe the solution thermodynamics of this system. Moreover, the reasonably low standard deviations in $\log\beta_{pqr}$'s and the low Hamilton R-factor give confidence to the proposed model used in the data analysis.

Potentiometric data analysis by ESTA gave four possible species MLH, ML, MLH_{-1} and MLH_{-2}. Because copper(II) forms coloured complexes with the ligand, the coordination geometries of the complex species present in solution have been confirmed by UV/Vis spectrophotometry. The spectra for MLH_{-2} is not observed because it was difficult to obtain spectra at pH>8. However, spectra were obtained for

three complex species and spectroscopic measurements indicate that Cu^{2+} sits in a square planar environment of nitrogen donor atoms in the MLH_{-1} species.

Zinc(II) and calcium(II) ions being present in blood plasma in large concentrations are regarded as potential competitors of copper(II) *in vivo*.[3,4] However, zinc(II) complexes are likely to predominate at physiological pH because of its high concentration and the ability to form complex species at this pH. From the pmi results, PCUA has been found to be a better copper mobilizing ligand as compared to 5UM which is also a diamino diamide ligand. However, the pmi of PCUA is still very low it to compete with other l.m.w. species in blood plasma. Moreover, Zn(II) and Ca(II) have been found to be competitors of copper(II) for PCUA in blood plasma.

NMR studies carried out supported protonation of PCUA and complexation with copper(II). The protonation of the amine nitrogens was observed as pH increased from 2-11. Therefore, influencing the chemical environment of the protons attached to carbons next to the amine groups. Upon complexation with copper(II), the observed peaks broadened and shifted, thus confirming complexation of PCUA with copper(II).

Although complex species of PCUA with copper(II) were found to have little plasma copper mobilizing ability, the results in a way contribute to further investigations of anti-arthritic agents. In order to increase stability of complex species, 5 and 6 membered rings should be maintained in chelate rings. Finally, the search for new ligands must continue.

References

1 Reichert D.E., Lewis J.S., Anderson C.J., *Coord. Chem. Rev.*, 1999, **184**, 3.

2 Laurie S.H., Mohammed E.S., *J. Chem. Soc. Dalton Trans.* 1995, 129.

3 Jackson G.E., Kelly M.J., *J. Chem. Soc. Dalton Trans.* 1989, 2429-2433.

4 Jackson G.E., Nakani B.S., *J. Chem. Soc. Dalton Trans.* 1996, 1373-1377.